

1 **A global 3-D CTM evaluation of black carbon in the Tibetan Plateau**

2 **C. He^{1,2}, Q. B. Li^{1,2}, K. N. Liou^{1,2}, J. Zhang³, L. Qi^{1,2}, Y. Mao^{1,2}, M. Gao^{1,2}, Z. Lu⁴,**
3 **D. G. Streets⁴, Q. Zhang⁵, M. M. Sarin⁶, K. Ram⁷**

4 1. Department of Atmospheric and Oceanic Sciences, University of California, Los
5 Angeles, CA, USA

6 2. Joint Institute for Regional Earth System Science and Engineering, University of
7 California, Los Angeles, CA, USA

8 3. Department of Atmospheric and Oceanic Sciences, School of Physics, Peking
9 University, Beijing, China

10 4. Decision and Information Sciences Division, Argonne National Laboratory,
11 Argonne, Illinois, USA

12 5. Center for Earth System Science, Tsinghua University, Beijing, China

13 6. Department of Geosciences, Physical Research Laboratory, Ahmedabad, India

14 7. Institute of Environment and Sustainable Development, Banaras Hindu University,
15 Varanasi, India

16 Correspondence to: C. He (cenlinhe@atmos.ucla.edu)

17

18 **Abstract**

19 We systematically evaluate the black carbon (BC) simulations for 2006 over the
20 Tibetan Plateau by a global 3-D chemical transport model (CTM) (GEOS-Chem)
21 driven by GEOS-5 assimilated meteorological fields, using *in situ* measurements of
22 BC in surface air, BC in snow, and BC absorption aerosol optical depth (AAOD).
23 Using improved anthropogenic BC emission inventories for Asia that account for
24 rapid technology renewal and energy consumption growth (Zhang et al., 2009; Lu et
25 al., 2011) and improved global biomass burning emission inventories that account for
26 small fires (van der Werf et al., 2010; Randerson et al., 2012), we find that model
27 results of both BC in surface air and in snow are statistically in good agreement with
28 observations (biases < 15%) away from urban centers. Model results capture the
29 seasonal variations of the surface BC concentrations at rural sites in the Indo-Gangetic
30 Plain, but the observed elevated values in winter are absent. Modeled surface BC
31 concentrations are within a factor of two of the observations at remote sites. Part of
32 the discrepancy is explained by the deficiencies of the meteorological fields over the

1 complex Tibetan terrain. We find that BC concentrations in snow computed from
2 modeled BC deposition and GEOS-5 precipitation are spatiotemporally consistent
3 with observations ($r = 0.85$). The computed BC concentrations in snow are a factor of
4 2-4 higher than the observations at several Himalayan sites because of excessive BC
5 deposition. The BC concentrations in snow are biased low by a factor of two in the
6 central Plateau, which we attribute to the absence of snow aging in the CTM and
7 strong local emissions unaccounted for in the emission inventories. Modeled BC
8 AAOD is more than a factor of two lower than observations at most sites, particularly
9 to the northwest of the Plateau and along the southern slopes of the Himalayas in
10 winter and spring, which is attributable in large part to underestimated emissions and
11 the assumption of external mixing of BC aerosols in the model. We find that
12 assuming a 50% increase of BC absorption associated with internal mixing reduces
13 the bias in modeled BC AAOD by 57% in the Indo-Gangetic Plain and the
14 northeastern Plateau and to the northeast of the Plateau, and by 16% along the
15 southern slopes of the Himalayas and to the northwest of the Plateau. Both surface BC
16 concentration and AAOD are strongly sensitive to anthropogenic emissions (from
17 China and India), while BC concentration in snow is especially responsive to the
18 treatment of BC aerosol aging. We find that a finer model resolution ($0.5^\circ \times 0.667^\circ$
19 nested over Asia) reduces the bias in modeled surface BC concentration from 15% to
20 2%. The large range and non-homogeneity of discrepancies between model results
21 and observations of BC across the Tibetan Plateau undoubtedly undermine current
22 assessments of the climatic and hydrological impact of BC in the region thus warrant
23 imperative needs for more extensive measurements of BC, including its concentration
24 in surface air and snow, AAOD, vertical profile and deposition.

25

26 **1. Introduction**

27 Black carbon (BC) is the most important light-absorbing aerosol formed during
28 incomplete combustion (Bond et al., 2013, and references therein), with major sources
29 from fossil fuel and biofuel combustion and open biomass burning (Bond et al., 2004).
30 BC warms the atmosphere by strongly absorbing solar radiation in the visible and the
31 near infrared (Ramanathan and Carmichael, 2008), influences cloud formation as
32 cloud condensation nuclei (Jacobson, 2006), and accelerates snow and ice melting by
33 significantly reducing snow and ice albedo (i.e., the snow-albedo effect) (Hansen and

1 Nazarenko, 2004; Flanner et al., 2007). With an estimated global climate forcing of
2 $+1.1 \text{ W m}^{-2}$, BC is now considered the second most important human emission in
3 terms of its climate forcing in the present-day atmosphere after carbon dioxide
4 (Ramanathan and Carmichael, 2008; Bond et al., 2013). The regional warming effect
5 of BC can be even stronger, particularly over snow-covered regions (Jacobson, 2004;
6 Flanner et al., 2007, 2009). There is ample evidence that BC aerosols deposited on
7 Tibetan glaciers have been a significant contributing factor to observed rapid glacier
8 retreat in the region (e.g., Xu et al., 2009). It has also been proposed that the radiative
9 forcing from ever-increasing deposition of BC in snow was an important cause for the
10 retreat of Alpine glaciers from the last little ice age through the mid-19th century
11 (Painter et al., 2013).

12 The Tibetan Plateau is the highest plateau in the world with the largest snow and ice
13 mass outside the polar regions (Xu et al., 2009). The Tibetan glaciers and the
14 associated snowmelt are the primary source of fresh water supply for drinking,
15 agricultural irrigation, and hydropower for more than one billion people in Asia
16 (Immerzeel et al., 2010). The Plateau also plays a critical role in regulating the Asian
17 hydrological cycle. Changes of snow cover affect heat flux and water exchange
18 between the surface and the atmosphere, and further disturb the formation of the
19 Asian monsoon (Lau and Kim, 2006).

20 Observations have shown remarkable warming and accelerated glacier retreat in the
21 Tibetan Plateau in the past decades (Qin et al., 2006; Prasad et al., 2009). Ramanathan
22 et al. (2005, 2007) argued that the ever-increasing amount of BC transported to the
23 Himalayas accounts for half of the observed warming in the region, comparable to the
24 warming attributable to greenhouse gases (Barnett et al., 2005). Recent studies
25 reaffirmed a strong BC-induced regional warming over the Plateau that results in
26 more than 1% decrease of snow/ice cover (Lau et al., 2010; Menon et al., 2010), 2~5%
27 reduction of snow albedo (Yasunari et al., 2010), and an increase of runoff in early
28 spring (Qian et al., 2011). Surrounded by the world's two largest BC source regions,
29 South and East Asia (Lamarque et al., 2010), the Plateau has received an increasing
30 BC deposition from 1951 to 2000, particularly after 1990 (Ming et al., 2008). Recent
31 studies have shown that the amount of BC transported to the Plateau has increased by
32 41% from 1996 to 2010, with South and East Asia accounting for 67% and for 17%

1 on an annual basis (Lu et al., 2012). The modeling study by Kopacz et al. (2011)
2 suggested that long-range transport from Middle East, Europe, and Northern Africa
3 also contributes to the BC deposition over the Plateau.

4 The climatic effects of BC over the Tibetan Plateau are not well understood, with
5 large uncertainties in the estimates of BC radiative forcing (e.g. Flanner et al., 2007;
6 Kopacz et al., 2011; Ming et al., 2013). Accurate assessment of BC-related radiative
7 forcing in the Tibetan Plateau critically depends on reliable model simulations of BC
8 emissions, transport and subsequent deposition, and vertical distribution over the
9 Plateau. Previous modeling studies have found invariably large discrepancies with
10 observations. For example, the simulations of surface BC at several sites in the
11 southern slope of the Himalayas are biased low by more than a factor of two,
12 particularly in winter and spring in regional, multi-scale and global models (Nair et al.,
13 2012; Moorthy et al., 2013). Fu et al. (2012) showed that a global chemical transport
14 model (CTM) simulated surface BC concentrations are more than 50% lower than
15 observations in China in general and across the Tibetan Plateau in particular. A global
16 CTM study (Kopacz et al., 2011) and a global climate model (GCM) study (Qian et
17 al., 2011) both showed large differences between modeled and observed BC
18 concentration in snow over the Plateau. Sato et al. (2003) and Bond et al. (2013)
19 pointed out large underestimates of BC absorption aerosol optical depth (AAOD) in
20 previous models compared with Aerosol Robotic Network (AERONET) retrievals.

21 In this study we seek to understand the capability of a global 3-dimentional CTM
22 (GEOS-Chem) in simulating BC in the Tibetan Plateau and the associated
23 discrepancies between model results and observations. The GEOS-Chem model has
24 been widely used in previous studies to understand BC emissions, transport and
25 deposition in the Plateau (Kopacz et al., 2011), in China (Fu et al., 2012), over Asia
26 (Park et al., 2005), in the Arctic (Wang et al., 2011) and globally (Wang et al., 2014).
27 To our knowledge, this is the first attempt to systematically evaluate a global
28 simulation of BC in the Tibetan Plateau using all three types of available *in situ*
29 measurements: BC in surface air, BC in snow, and BC AAOD. We further delineate
30 the effects of anthropogenic BC emissions from China and India, BC aging process
31 and model resolution on the simulation. Potential factors driving model versus
32 observation discrepancies are also examined, which gives implications for improving

1 the estimate of BC climatic effects. Observations and model description are presented
2 in Sect. 2. Simulations of surface BC, BC in snow and BC AAOD are discussed in
3 Sect. 3. Sensitivity and uncertainty analyses are in Sects. 4, 5 and 6. Finally, summary
4 and conclusions are given in Sect. 7.

5 **2. Method**

6 **2.1 Observations**

7 For the sake of clarity, we define here the Tibetan Plateau roughly as the region in
8 28°N-40°N latitudes and 75°E-105°E longitudes. We also define several sub-regions
9 of the Plateau and adjacent regions (Fig. 1): the central Plateau (30°N-36°N, 82°E-
10 95°E), the northwestern Plateau (36°N-40°N, 75°E-85°E), the northeastern Plateau
11 (34°N-40°N, 95°E-105°E), the southeastern Plateau (28°N-34°N, 95°E-105°E), to the
12 north of the Plateau (40°N-50°N, 85°E-95°E), to the northwest of the Plateau (40°N-
13 50°N, 70°E-85°E), to the northeast of the Plateau (40°N-50°N, 95°E-105°E), and the
14 Himalayas. There are rather limited measurements of BC in the Tibetan Plateau. Fig.
15 1 shows sites with measurements of BC surface concentration, concentration in snow,
16 and AAOD in the region.

17 **2.1.1 BC surface concentration**

18 There are 13 sites with monthly or seasonal measurements of surface BC
19 concentration (Table 1 and Fig. 1). Observations are available for 2006 at nine of the
20 sites. Four sites provide observations for 1999-2000, 2004-2005 or 2008-2009. We
21 distinguish these sites as urban, rural, or remote sites based upon annual mean surface
22 BC concentration, following Zhang et al. (2008). The concentration is typically higher
23 than $5 \mu\text{g m}^{-3}$ at urban sites (within urban centers or near strong local residential and
24 vehicular emissions), in the range of $2-5 \mu\text{g m}^{-3}$ at rural sites, and less than $2 \mu\text{g m}^{-3}$ at
25 more remote, pristine sites.

26 Ganguly et al. (2009b) retrieved surface BC concentration at Gandhi College (25.9°N,
27 84.1°E, 158 m a.s.l.) by combining aerosol optical properties from AERONET
28 measurements and aerosol extinction profiles from Cloud-Aerosol Lidar with
29 Orthogonal Polarization (CALIOP) observations. The retrieval is rather sensitive to
30 errors in the aerosol single scattering albedo, size distribution and vertical profiles
31 derived from the observations (Ganguly et al., 2009a). Measurements at Delhi

1 (28.6 °N, 77.2 °E, 260 m a.s.l.), Digrugarh (27.3 °N, 94.6 °E, 111 m a.s.l.), Kharagpur
2 (22.5 °N, 87.5 °E, 22 m a.s.l.) and Nepal Climate Observatory at Pyramid (NCOP,
3 28.0 °N, 86.8 °E, 5079 m a.s.l.) used Aethalometer (Beegum et al., 2009; Pathak et al.,
4 2010) or Multi-angle Absorption Photometer (Bonasoni et al., 2010; Nair et al., 2012).
5 The uncertainties of these measurements stem mainly from the interference from
6 other components in the aerosol samples (Bond et al., 1999; Petzold and Schonlinner,
7 2004) and the shadowing effects under high filter loads (Weingartner et al., 2003). BC
8 concentrations at the other sites were derived from measurements of the Thermal
9 Optical Reflectance or Thermal Optical Transmittance (Carrico et al., 2003; Qu et al.,
10 2008; Zhang et al., 2008; Ming et al., 2010; Ram et al., 2010a,b). These
11 measurements are strongly influenced by the temperature chosen to separate BC and
12 organic carbon (OC) (Schmid et al., 2001; Chow et al., 2004).

13 **2.1.2 BC concentration in snow**

14 There are 16 sites with monthly or seasonal measurements of BC concentration in
15 snow during 1999-2007 and two with annual measurements (Xu et al., 2006, 2009;
16 Ming et al., 2009a, b, 2012, 2013). These sites are at high-elevation (> 3500 m a.s.l.),
17 remote locations in the Himalayas and other parts of the Plateau (Table 2 and Fig. 1).
18 The snow and ice samples taken from these sites were heated and filtered through
19 fiber filters in the laboratory. Thermal techniques (Cachier and Pertuisot, 1994; Chow
20 et al., 2004) were then used to isolate BC from other constituents (especially OC) in
21 the filters, followed by analysis using carbon analyzers including heating-gas
22 chromatography (Xu et al., 2006), optical carbon analysis (Chow et al., 2004) and
23 coulometric titration-based analysis (Cachier and Pertuisot, 1994). The accuracy of
24 the heating-gas chromatography system is dominated by the variability of the blank
25 loads of pre-cleaned filters (Xu et al., 2006). The coulometric titration-based analysis
26 measures the acidification of the solution by carbon dioxide produced from BC
27 combustion in the system (Ming et al., 2009a), where the pH value of the solution
28 may be interfered by other ions.

29 **2.1.3 AERONET AAOD**

30 There are 14 AERONET sites with AAOD retrievals in the Tibetan Plateau and
31 adjacent regions (Table 3 and Fig. 1). These sites are mostly in the Indo-Gangetic

1 Plain, in northern India and along the southern slope of the Himalayas. Following
2 Bond et al. (2013), we infer BC AAOD from monthly averaged AOD data from
3 AERONET (Version 2.0 Level 2.0 products) for 2006-2012. The monthly means are
4 derived for months when there are five or more days with AOD observations. The
5 measurements provide sun and sky radiance observations in the mid-visible range
6 (Dubovik and King, 2000), which allows for inference of aerosol column absorption
7 from retrievals of AOD and single scattering albedo (SSA) via $\text{AAOD} = \text{AOD} \times (1 -$
8 $\text{SSA})$. As pointed out by Bond et al. (2013), the removal of SSA data at low AOD
9 values from the AERONET data (for data quality assurance) likely introduces a
10 positive bias in the AAOD retrieval. Both BC aerosols and dust particles contribute to
11 the absorption. The absorption by fine-mode aerosols is primarily from BC while the
12 absorption by larger particles (diameter $> 1 \mu\text{m}$) is principally from dust. Dust AAOD
13 is estimated from the super-micron part of aerosol size distribution provided by the
14 AERONET retrieval method and a refractive index of $1.55 + 0.0015i$ (Bond et al.,
15 2013). BC AAOD is then the difference between the total and dust AAOD. This
16 process attributes all fine-mode aerosol absorption to BC. Because of the
17 contributions from OC and fine dust particles to fine-mode AAOD, the inferred BC
18 AAOD is likely biased high. Bond et al. (2013) estimated that the uncertainty from
19 the impact of dust and OC on the fine-mode AAOD could be as large as 40-50%. The
20 limited AERONET sampling in this region is another source of uncertainty (Bond et
21 al., 2013).

22 **2.2 Model description and simulations**

23 The GEOS-Chem model is driven by assimilated meteorology from the Goddard
24 Earth Observing System (GEOS) of the NASA Global Modeling and Assimilation
25 Office (GMAO). We use here GEOS-Chem version 9-01-03 (available at <http://geos-chem.org>), driven by GEOS-5 data assimilation system (DAS) meteorological fields.
26 The meteorological fields have a native horizontal resolution of $0.5^\circ \times 0.667^\circ$, 72
27 vertical layers, and a temporal resolution of 6 hours (3 hours for surface variables and
28 mixing depths). The spatial resolution is degraded to $2^\circ \times 2.5^\circ$ in the horizontal and
29 47 layers in the vertical (from the surface to 0.01 hPa) for computational expediency.
30 The lowest model levels are centered at approximately 60, 200, 300, 450, 600, 700,
31 850, 1000, 1150, 1300, 1450, 1600, 1800 m a.s.l.

1 Tracer advection is computed every 15 minutes with a flux-form semi-Lagrangian
2 method (Lin and Rood, 1996). Tracer moist convection is computed using GEOS
3 convective, entrainment, and detrainment mass fluxes as described by Allen et al.
4 (1996a, b). The deep convection in GEOS-5 is parameterized using the relaxed
5 Arakawa-Schubert scheme (Arakawa and Schubert, 1974; Moorthi and Suarez, 1992),
6 and the shallow convection treatment follows Hack (1994). Park et al. (2003, 2006)
7 first described GEOS-Chem simulation of carbonaceous aerosols.

8 **2.2.1 BC emissions**

9 The global anthropogenic BC emissions are from Bond et al. (2007), with an annual
10 emission of 4.4 Tg C for the year 2000. Anthropogenic BC emissions in Asia, chiefly
11 in China and India, have increased significantly since 2000 (Granier et al., 2011).
12 Zhang et al. (2009) developed an Asian anthropogenic BC emissions (for China and
13 India and the rest of Asia) for 2006 for the Intercontinental Chemical Transport
14 Experiment-B (INTEX-B) field campaign (Singh et al., 2009), with considerable
15 updates to a previous inventory developed by Streets et al. (2003). They employed a
16 dynamic methodology that accounts for rapid technology renewal and updated the
17 fuel consumption data. Fu et al. (2012) pointed out that Zhang et al. (2009)
18 underestimates anthropogenic BC emissions in China by a factor of 1.6 compared
19 with the top-down estimates. Lu et al. (2011) further updated the activity rates,
20 technology penetration data and emission factors in China and India, and reported
21 anthropogenic BC emissions only in these two countries for 1996-2010. Table 4 is a
22 summary of the two inventories. Anthropogenic BC emissions in India are lower in
23 the Zhang et al. (2009) inventory (hereinafter the INTEX-B inventory) than in the Lu
24 et al. (2011) inventory (hereinafter the LU inventory) by a factor of two, while
25 emissions in China are 10% higher in the INTEX-B inventory than in the LU
26 inventory (Table 4). The higher emissions in India in the LU inventory are primarily a
27 result of the updated biofuel emission factors and the new method used to estimate
28 biofuel consumptions. The biofuel emissions, which are dominated by residential
29 burning, account for more than 50% of total BC emissions in India (Lu et al., 2011).
30 There are large uncertainties in both inventories. Lu et al. (2011) used a Monte Carlo
31 method to show that the 95% uncertainty ranges of BC emissions are from -43% to 93%
32 for China and from -41% to 87% for India. The uncertainties in the INTEX-B
33 inventory are $\pm 208\%$ for China and $\pm 360\%$ for India (Zhang et al., 2009). A recent

1 study by Qin and Xie (2012) showed slightly (5-10%) lower total anthropogenic BC
2 emissions in China than those from Lu et al. (2011) for 2006 but a factor of 2 higher
3 emissions in the northeastern and northwestern China. Kurokawa et al. (2013) further
4 updated BC emissions in Asia and found 10% lower anthropogenic BC emissions for
5 China and 30% lower for India compared with those from Lu et al. (2011), yet with a
6 similar spatial distribution. Wang et al. (2014) developed a new global BC emission
7 inventory, where anthropogenic BC emissions are 20% higher in China and 30%
8 lower in India than those from Lu et al. (2011). They found that the use of the new
9 inventory reduces model biases of surface BC concentrations in Asia by 15-20%.
10 However, the abovementioned three latest inventories are still associated with large
11 uncertainties (95% confidence intervals), which are more than 100% for
12 anthropogenic BC emissions in China and India (Qin and Xie, 2012; Kurokawa et al.,
13 2013; Wang et al., 2014).

14 Global biomass burning emissions are from the Global Fire Emissions Database
15 version 3 (GFEDv3) (van der Werf et al., 2010). Kaiser et al. (2012) showed that
16 GFEDv3 underestimates carbon emissions by a factor of 2-4 globally because of
17 undetected small fires. Randerson et al. (2012) reported an updated GFEDv3
18 inventory that accounts for small fire emissions. Small fires increase carbon emissions
19 by 50% in Southeast Asia and Equatorial Asia (Randerson et al., 2012). We use the
20 GFEDv3 emissions with a monthly temporal resolution in the present study. The
21 uncertainty of the GFEDv3 emissions is at least 20% globally and higher in boreal
22 regions and Equatorial Asia (van der Werf et al., 2010). The major uncertainty lies in
23 insufficient data on burned area, fuel load and emission factor (van der Werf et al.,
24 2010; Randerson et al., 2012).

25 **2.2.2 BC deposition**

26 Simulation of aerosol dry and wet deposition follows Liu et al. (2001). Dry deposition
27 of aerosols uses a resistance-in-series model (Walcek et al., 1986) dependent on local
28 surface type and meteorological conditions. There have since been many updates. A
29 standard resistance-in-series scheme (Wesely, 1989) has been implemented in the
30 non-snow/non-ice regions (Wang et al., 1998) with a constant aerosol dry deposition
31 velocity of 0.03 cm s^{-1} prescribed over snow and ice (Wang et al., 2011). This
32 velocity is within the range ($0.01\text{--}0.07 \text{ cm s}^{-1}$) employed in Liu et al. (2011) to

1 improve the BC simulation in the Geophysical Fluid Dynamics Laboratory (GFDL)
2 Atmospheric Model version 3 (AM3) global model (Donner et al., 2011). We found
3 that dry deposition accounts for 20% of the total BC deposition over the Tibetan
4 Plateau in winter and 10% in summer.

5 Liu et al. (2001) described the wet scavenging scheme for aerosols in the GEOS-
6 Chem. Wang et al. (2011) implemented in the model a new below-cloud scavenging
7 parameterization for individual aerosol mode, which distinguishes between the
8 removal by snow and by rain drops for aerosol washout. They also applied different
9 in-cloud scavenging schemes to cold and to warm clouds, and with an improved areal
10 fraction of a model grid box that experiences precipitation. These changes are
11 included in the GEOS-Chem version used for the present study.

12 The GEOS-Chem model does not directly predict BC (or any aerosols for that matter)
13 in snow at the surface in the absence of a land-surface model that explicitly treats
14 snow including its aging. As an approximation, we estimate BC concentration in snow
15 in the model as the ratio of total BC deposition to total precipitation, following
16 Kopacz et al. (2011) and Wang et al. (2011). Although the use of total precipitation
17 here is reasonable considering the low temperature typical over the Tibetan Plateau
18 (Wu and Liu, 2004), it introduces uncertainties to the calculation of snow BC
19 concentration. Bonasoni et al. (2010) found that precipitation can be partly in the form
20 of rain even at altitudes of 5 km in the Himalayas. Thus, the use of total precipitation
21 may overestimate both snow precipitation and BC removed by snow. Besides, rain
22 also results in the melting of snowpack (Marks et al., 2001), which further affects BC
23 concentration in snow. Additional uncertainties exist in the GEOS-5 precipitation
24 fields because of the coarse model resolution and the complex topography in the
25 Plateau (see Sect. 3.2). Ménégoz et al. (2013) showed that using a higher resolution
26 model ($0.2^\circ \times 0.2^\circ$) improves the simulation of the spatial variability of precipitation in
27 the Himalayas, but the bias in total precipitation remains high. The uncertainty in
28 precipitation is thus propagated to the BC concentration in snow computed from
29 model results. Our calculation of BC concentration in snow assumes a well mixing of
30 BC and snow. However, BC content is not uniform throughout a snow column. Thus,
31 an ideal comparison of modeled and observed BC concentrations in snow should be
32 for the same depth of a snow column. We also neglect the aging of surface snow and

1 the internal mixing of snow and BC, which conceivably contribute to the
2 underestimate of BC concentration in snow computed here. This may be an especially
3 important issue for comparisons in the central Plateau and to the north of the Plateau,
4 where snowmelt has been suggested to strongly increase BC concentration in snow
5 (Zhou et al., 2007; Ming et al., 2013).

6 **2.2.3 BC aging**

7 Freshly emitted BC is mostly (80%) hydrophobic (Cooke et al., 1999). Hydrophobic
8 BC becomes hydrophilic typically on the timescale of a few days (McMeeking et al.,
9 2011 and references therein), because of coating by soluble materials like sulfate and
10 organic matter (Friedman et al., 2009; Khalizov et al., 2009). The internal mixing of
11 BC and other aerosol constituents significantly changes the morphology,
12 hygroscopicity and optical properties of BC particles (Zhang et al., 2008). This further
13 influences BC absorption efficiency (Bond et al., 2006) and lifetime against
14 deposition (Mikhailov et al., 2001). However, the aging process is not explicitly
15 simulated in the GEOS-Chem, where an e-folding time of 1.15 days for the
16 conversion of hydrophobic to hydrophilic BC is simply assumed (Park et al., 2005;
17 Kopacz et al., 2011; Wang et al., 2011). Liu et al. (2011) proposed a condensation-
18 coagulation parameterization for BC aging where the conversion time is not uniform
19 but varies. Specifically, the conversion is assumed to be primarily a result of sulfuric
20 acid deposition (condensation) onto BC particles and the mass deposition rate is
21 proportional to the concentration of gaseous sulfuric acid and to the BC particle
22 surface area. Gaseous atmospheric sulfuric acid is a product of sulfur dioxide
23 oxidation by the hydroxyl radical (OH). Consequently its steady-state concentration is
24 linearly linked to OH concentration. Thus, in the absence of nucleation, which is a
25 slow process when there exists plenty of primary particles as found in urban and
26 biomass burning plumes (Seinfeld and Pandis, 2006), the BC aging rate can be
27 parameterized as a linear function of OH concentration, where the coefficient of OH
28 concentration controls a fast aging process (i.e. condensation) and the constant term
29 governs a slow aging process (e.g. coagulation). Huang et al. (2013) further combined
30 the Liu et al. (2011) parameterization with a chemical oxidation aging mechanism
31 from chamber study results (Poschl et al., 2001) in GEOS-Chem. They found that the
32 chemical aging effects on surface BC concentrations are strongest in the tropical
33 regions but negligible over the Tibetan Plateau.

1 **2.2.4 Model simulations**

2 For the present study, we conducted four GEOS-Chem simulations for 2006 (Table 5).
3 Detailed discussions and justifications for these model experiments are provided
4 below where appropriate. Model results are sampled at the corresponding locations of
5 the measurement sites. Model results presented here are monthly averages. As pointed
6 out in previous studies (Fairlie et al., 2007; Mao et al., 2011), comparing localized
7 observations with model results that are representative of a much larger area is
8 inherently problematic. The mountainous sites and the complex terrain in the Tibetan
9 Plateau further complicate the comparison.

10 In Experiment A, we replace the Bond et al. (2007) emissions in China and India with
11 the LU inventory and use the INTEX-B inventory for the rest of Asia. This is our
12 standard simulation and the results are used for all model evaluations presented here
13 unless stated otherwise. We also provide the model results from Experiment A but
14 instead using the lower and upper bounds of anthropogenic BC emissions from China
15 and India estimated by Lu et al. (2011). We find that wet deposition accounts for 83%
16 of the global annual BC deposition, consistent with the previous results of $78.6 \pm 17\%$
17 from the Aerosol inter-Comparison project (AeroCom) multi-model study (Textor et
18 al., 2006). The tropospheric lifetime of BC against deposition is 5.5 days, at the lower
19 end of the range (5-11 days) reported by Koch et al. (2009). The difference between
20 Experiments B and A is that we replace the Bond et al. (2007) emissions in China and
21 India with the INTEX-B inventory in Experiment B. By contrasting model results
22 from these two experiments, we aim to assess the sensitivity of BC in the Tibetan
23 Plateau to changes in the anthropogenic emissions from India and China, the two
24 largest source regions of BC to the Plateau (Kopacz et al., 2011; Lu et al., 2012), as
25 will be discussed in further details in Sect. 4. Both Experiments A and B use an e-
26 folding time of 1.15 days for BC aging. Experiment C applies the Liu et al. (2011)
27 parameterization for BC aging instead. We used monthly mean OH concentrations
28 with diurnal variations in the parameterization, which is derived from the offline
29 GEOS-chem simulation with the same spatial resolution as BC simulations. The
30 resulting e-folding time is 2.5 days on average globally and 2 days in Asia. The longer
31 e-folding time results in longer atmospheric lifetime, larger deposition and higher
32 hydrophobic fraction of BC over the Tibetan Plateau (not shown). We discuss further
33 in Sect. 5 the differing results between Experiments C and A, which allow us to

1 appraise the effect of a variable BC aging time on BC in the Plateau. In Experiment D,
2 we replace the model resolution of $2^\circ \times 2.5^\circ$ used in Experiment A with a finer
3 resolution of $0.5^\circ \times 0.667^\circ$ nested over Asia (11°S - 55°N , 70°E - 150°E). The differences
4 between the results from Experiments D and A will be discussed in Sect. 6 for the
5 purpose of evaluating the impact of model resolution on BC in the Plateau. In all
6 model experiments, we use a BC mass absorption cross section (MAC) of $7 \text{ m}^2 \text{ g}^{-1}$
7 from observations (Clarke et al., 2004) for calculating modeled BC AAOD. We note
8 that BC MAC is associated with large uncertainties, which varies from 3 to $25 \text{ m}^2 \text{ g}^{-1}$
9 depending on atmospheric conditions (Bond and Bergstrom, 2006).

10 **3. Results**

11 **3.1 BC in surface air**

12 Fig. 2 shows surface BC concentrations at Kharagpur (22.5°N , 87.5°E , 28 m a.s.l., Fig.
13 2a), Gandhi College (25.9°N , 84.1°E , 158 m a.s.l., Fig. 2b) and Kanpur (26.4°N ,
14 80.3°E , 142 m a.s.l., Fig. 2c), three rural sites. Model results reproduce the observed
15 BC concentrations with the exception of winter, when the model underestimates the
16 concentrations by 50%. The high wintertime concentrations are primarily because of
17 emissions from agricultural waste and wood fuel burning that is dominant over the
18 Indo-Gangetic Plain during winter (Ram et al., 2010b). Model results using the upper
19 bound of BC emissions capture the observed high concentrations in winter (Fig. 2a-c).
20 The wintertime low biases in the model therefore clearly call for enhanced emission
21 estimates. Moorthy et al. (2013) found that modeled surface BC concentrations in this
22 region are underestimated by more than a factor of two during winter when the
23 planetary boundary layer (PBL) is convectively stable, while model underestimates
24 are smaller in summer when the PBL is unstable. They suggested that the
25 overestimate of wintertime PBL height in chemical transport models is an important
26 contributor to model underestimates of surface pollutant concentrations. Lin and
27 McElroy (2010) pointed out that the assumption of full PBL mixing (instantaneous
28 vertical mixing throughout the mixing depth) in the GEOS-Chem tends to
29 overestimate vertical mixing under a stable PBL condition. They proposed and
30 implemented in GEOS-Chem a non-local PBL mixing scheme (Holtslag and Boville,
31 1993; Lin et al., 2008), where the mixing states are determined by static instability.
32 They used a local K-theory scheme (Louis, 1979) for a stable PBL and added a “non-

1 local” term for an unstable PBL to account for the PBL-wide mixing triggered by
2 large eddies. Our results show that the non-local boundary layer mixing increases
3 surface BC concentrations by up to 25% in winter and spring, a significant
4 improvement. Nair et al. (2012) showed that the non-local boundary layer mixing still
5 tends to overestimate the vertical mixing during winter in the Indo-Gangetic Plain.

6 Model results are within $\pm 50\%$ of the observations at two remote sites, Zhuzhang
7 (28.0°N, 99.7°E, 3583 m a.s.l., Fig. 2h) and NCOS (30.8°N, 91.0°E, 4730 m a.s.l., Fig.
8 2i), where observations are available for only fall and winter. Model results are lower
9 than the observations at NCOP (28.0°N, 86.8°E, 5079 m a.s.l., Fig. 2g) and Nagarkot
10 (27.7°N, 85.5°E, 2150 m a.s.l., Fig. 2e) by a factor of two in spring. Using the upper
11 bound of BC emissions captures the springtime high concentrations at Nagarkot but
12 not at NCOP (Fig. 2g, e). The two sites are influenced by emissions from nearby
13 Nepal valleys transported by the mountain-valley wind (Carrico et al., 2003; Bonasoni
14 et al., 2010). In contrast, model results capture the relatively high concentrations in
15 winter and spring observed at Manora Peak (29.4°, 79.5°E, 1950 m a.s.l., Fig. 2d) and
16 Langtang (28.1°N, 85.6°E, 3920 m a.s.l., Fig. 2f), but overestimate the summertime
17 concentrations by a factor of two. Using the lower bound of BC emissions is still not
18 able to capture the observed low values in summer (Fig. 2d, f). Part of the
19 discrepancies is explained by the inherent difficulty in simulating the meteorological
20 fields over the complex Himalayan terrain. Chen et al. (2009) showed that the terrain
21 effects and meteorological features in the Tibetan Plateau are not entirely reproduced
22 by the GEOS-5 meteorological fields. Such difficulty is not unique to the Himalaya
23 region. Emery et al. (2012) also showed that the transport of chemical species is not
24 well simulated over the complex terrain in the western U.S. using GEOS-Chem driven
25 by GEOS-5 meteorological fields $2^\circ \times 2.5^\circ$.

26 Surface concentrations of BC at Lhasa and Delhi, two urban sites (see Table 1), are
27 strongly affected by emissions from city traffic and industries (Zhang et al., 2008;
28 Beegum et al., 2009). The BC concentrations at Dibrugarh are highly impacted by the
29 emissions from the oil wells upwind and vehicular emissions from national highways
30 nearby (Pathak et al., 2010). The concentrations at Dunhuang, a well-known tourist
31 attraction and archaeological site, likely reflect vehicular emissions associated with
32 tourist traffic including tour buses. All four sites are characterized by strong local

1 emissions. Model results reproduce the seasonal trends at these “urban” sites (sites
2 that are near urban centers or heavily influenced by local emissions), but are low by
3 an order of magnitude (Fig. 3). Using the upper bound of BC emissions results in
4 doubling BC concentrations (Table 1), which by itself still cannot fully explain the
5 model versus observation discrepancies. We exclude these four urban sites from
6 analysis hereinafter.

7 There is a small negative bias of $-0.3 \text{ } \mu\text{g m}^{-3}$ in model simulated surface BC
8 concentrations (Fig. 4, left column), and the difference between model results and the
9 observations is statistically insignificant. We note that the residual errors at very low
10 BC concentrations may not be particularly meaningful. Overall, model results
11 reproduce the spatiotemporal variation of surface BC concentration throughout the
12 Tibetan Plateau ($r = 0.9$, root-mean-square-error RMSE = $1.3 \text{ } \mu\text{g m}^{-3}$) with the
13 exception of peak values (Fig. 4).

14 **3.2 BC in snow**

15 BC deposition and precipitation together determine BC concentration in snow, which
16 we approximate as the ratio of total BC deposition to total precipitation (see Sect.
17 2.2.2). Fig. 5 shows GEOS-Chem simulated annual mean BC deposition and GEOS-5
18 precipitation over Asia. The largest BC deposition over the Tibetan Plateau is in the
19 Himalayas and the southeastern Plateau (Fig. 5a), reflecting the proximity of strong
20 BC sources in northern India and southwestern China (Lu et al., 2012) and the intense
21 precipitation in the region (Fig. 5b). The northern Plateau is heavily influenced by BC
22 transported in the westerlies (Kopacz et al., 2011; Lu et al., 2012), but the lack of
23 strong precipitation (Fig. 5b) results in considerably smaller BC deposition (Fig. 5a).

24 Table 2 shows BC concentrations in snow at 18 sites across the Plateau. The
25 concentrations are 30% lower during the monsoon season (June – September) than
26 during the non-monsoon seasons (October – May), both in the observations and in the
27 model. Here the monsoon and non-monsoon seasons are defined following Xu et al.
28 (2009). The lowest BC concentrations in snow (minimum of $4.3 \text{ } \mu\text{g kg}^{-1}$) are in the
29 northern slope of the Himalayas, while the highest values (maximum of $141 \text{ } \mu\text{g kg}^{-1}$)
30 are to the north of the Plateau. Such spatial variation largely reflects the varying
elevations of the sites. Ming et al. (2009a, 2013) have shown that observed BC

1 concentration in snow over the Tibetan Plateau is inversely correlated with the
2 elevation of a site, with lower concentrations at higher elevations. Our model results
3 capture this spatial variation, but deviate from the observed concentrations by more
4 than a factor of two at several sites in the Himalayas and the central Plateau (Table 2).

5 Model results overestimate BC concentrations in snow during the monsoon season by
6 a factor of 2-4 at three Himalayan sites, Zuoqiupu (29.2°N, 96.9°E, 5500 m a.s.l.),
7 East Rongbuk (28.0°N, 87.0°E, 6500 m a.s.l.) and Namunani (30.4°N, 81.3°E, 5900
8 m a.s.l.) (Fig. 6). Model results using the lower bound of BC emissions still
9 overestimate the concentrations at these three sites (Table 2). Wet scavenging
10 accounts for more than 80% of the BC deposition over the Tibetan Plateau during the
11 monsoon season in the model. The large overestimate implies either excessive wet
12 deposition or inadequate precipitation or both in the Himalayas, given that BC
13 concentration in snow is approximated here as the ratio of BC deposition to
14 precipitation (see Sect. 2.2.2). Fig. 7 shows the monthly precipitation over different
15 parts of the Tibetan Plateau from the Global Precipitation Climatology Project (GPCP,
16 Huffman et al., 2001), the NOAA Climate Prediction Center (CPC) Merged Analysis
17 of Precipitation (CMAP, Xie and Arkin, 1997), the University of East Anglia Climate
18 Research Unit (CRU, Harris et al., 2014) and GEOS-5. GPCP precipitation is
19 generally consistent with that from CMAP in most parts of the Plateau except the
20 southeastern Plateau, where it is stronger by more than a factor of two. CRU
21 precipitation tends to be much stronger than those from GPCP and CMAP during the
22 monsoon season, particularly in the southeastern Plateau and the Himalayas (Fig. 7).
23 Previous studies have shown that the monsoon precipitation in the Himalayas is too
24 weak in both GPCP and CMAP data (Kitoh and Kusunoki, 2008; Voisin et al., 2008)
25 yet too strong in the CRU data (Zhao and Fu, 2006; Xie et al., 2007). The scarcity of
26 observational sites and the complex terrain of the Himalayas are two of the principle
27 reasons for large uncertainties in different precipitation datasets and apparent
28 inconsistencies among them (Ma et al., 2009; Andermann et al., 2011). Fig. 7 shows
29 that GEOS-5 precipitation is stronger than GPCP and CMAP data by a factor of two
30 in the Himalayas during the monsoon season. To probe the sensitivity of BC
31 deposition and our calculated BC concentration in snow in the Himalayas to
32 precipitation, we conducted a GEOS-Chem simulation where we reduced GEOS-5
33 precipitation in the region by 20% during the monsoon season. The resulting BC wet

1 deposition is only slightly lower (up to 5%), rather insensitive to changes in
2 presumably already intense precipitation during the monsoon season in the region.
3 This lack of strong sensitivity reflects an already efficient wet scavenging of BC in
4 the intense monsoon precipitation. The resulting BC concentrations in snow are
5 higher by 18% on average in the region, because the reduced precipitation tends to
6 concentrate BC in snow. Therefore, model overestimates of BC concentration in snow
7 in the region are less likely resulting from excessive monsoon precipitation but more
8 likely from excessive BC deposition. This is likely a result of overlong BC lifetime
9 due to insufficient wet removal. Wang et al. (2014) compared GEOS-Chem simulated
10 atmospheric BC concentrations with the HIAPER Pole-to-Pole Observations (HIPPO)
11 aircraft measurements and concluded that wet scavenging in the model is too weak.
12 This is in part because of the underestimated scavenging efficiency of BC in the
13 model. In addition, the relatively long BC aging time used in the model is also
14 potentially contributing to the weak wet scavenging. Recent observations suggest that
15 the e-folding time of about one day, for the hydrophobic-to-hydrophilic conversion of
16 BC, typically used in global models is too long (Akagi et al., 2012). The uncertainties
17 in wet scavenging in the model reduce the accuracy in the estimates of snow BC
18 concentrations. Excessive BC deposition can in part result from too strong PBL
19 mixing in the source regions and consequently excessive BC being transported into
20 the free troposphere. Our model results show that the non-local boundary layer
21 mixing (Lin and McElroy, 2010) reduces BC wet deposition by up to 5% on average
22 in the Himalayas during the monsoon season.

23 Fig. 6 shows that our calculated BC concentrations in snow are lower than
24 observations by a factor of two across the central Plateau. Model results using the
25 upper bound of BC emissions are able to reproduce the high BC concentrations in
26 snow at La'nong but miss those high values at the other sites (Table 2). Ming et al.
27 (2009a) pointed out that this region is predominantly influenced by biofuel burning
28 (residential cooking and heating) and biomass burning from religious activities. These
29 local emissions are largely unaccounted for in current emission inventories (Wang et
30 al., 2012). In addition, it is likely that the lack of consideration of snow aging also
31 lowers the BC concentration in snow computed here (Xu et al., 2006). We choose to
32 exclude Meikuang and Zhadang from the comparison here on account of local
33 emissions from coal-containing rock strata at the former (Xu et al., 2006) and strong

1 snow melting at the latter (Zhou et al., 2007). GEOS-5 precipitation in the central
2 Plateau is in general agreement with those from CMAP and CRU during the non-
3 monsoon season and that from GPCP during the monsoon season (Fig. 7e).

4 Model results are consistent with observations at the elevated sites in the northwestern
5 and northeastern Plateau and to the north of the Plateau (Fig. 6), where free
6 tropospheric BC is primarily northern mid-latitude pollution transported by the
7 westerlies (Kopacz et al., 2011; Lu et al., 2012). Regional emissions from western and
8 central China also contribute to BC deposition in these regions (Lu et al., 2012).
9 Although precipitation in these regions is weaker in GEOS-5 than in GPCP and
10 CMAP (Fig. 7b, d), previous studies have shown that GPCP and CMAP precipitation
11 is likely too strong there (Voisin et al., 2008; Ma et al., 2009).

12 Overall model results of BC concentration in snow have a small negative bias but a
13 large RMSE (Fig. 4, middle column), the latter results from the large discrepancies in
14 the Himalayas and the central Plateau. Model results are statistically in good
15 agreement with observations and reproduce the observed spatiotemporal variation ($r =$
16 0.85).

17 **3.3 BC AAOD**

18 Modeled BC AAOD is consistently lower than AERONET retrievals at most sites on
19 both a monthly (Fig. 4, right column) and an annual bases (Table 3). The annual mean
20 modeled BC AAOD over the Tibetan Plateau is 0.002 (Fig. 8), considerably lower
21 than the observations. Model results somewhat capture the observed spatial and
22 seasonal trends ($r = 0.53$), but to varying degrees underestimate the magnitudes (Fig.
23 9). Forty percent of the data points are too low by more than a factor of two in the
24 model, particularly in the Himalayas and to the northwest of the Plateau during winter
25 and spring when emissions are larger (relative to emissions during the rest of the year).
26 Most AERONET measurements in and around the Plateau are after 2006, whereas our
27 model results are for 2006. BC emissions in India have increased by $3.3\% \text{ yr}^{-1}$ since
28 2006 (Lu et al., 2011). Therefore, the large low bias in part reflects the
29 abovementioned temporal (hence emissions) mismatch. Using the upper bound of BC
30 emissions reduces the model versus observations discrepancies at six sites (Table 3),
31 but model results are still lower by a factor of two than the observed high AAODs at

1 the other sites. We also note that there are large uncertainties in the AERONET
2 AAOD retrieval (Bond et al., 2013), and that BC AAOD data is only scarcely
3 available in the Plateau and adjacent regions.

4 Another equally important factor contributing to the large discrepancy is the
5 assumption of external mixing of BC in the model, which leads to a weaker BC
6 absorption (Jacobson, 2001). Previous studies have found that BC absorption is
7 enhanced by 50% because of internal mixing (Bond et al., 2006). We find that a 50%
8 increase of BC absorption (using a MAC of $11 \text{ m}^2 \text{ g}^{-1}$ in our calculation) would
9 reduce the model bias by 57% in the Indo-Gangetic Plain and the northeastern Plateau
10 and to the northeast of the Plateau, and by 16% along the southern slopes of the
11 Himalayas and to the northwest of the Plateau (Fig. 9, right panel). There is evidence
12 that the enhancement of BC absorption due to internal mixing may be considerably
13 smaller than previously thought (Cappa et al., 2012). It is clear that the large
14 discrepancy (more than a factor of two) in the Himalayas and to the northwest of the
15 Plateau cannot be fully explained by the lack of BC internal mixing consideration
16 (and the associated larger absorption) in the model. Bond et al. (2013) pointed out that
17 current models significantly underestimate BC AAOD, particularly in South and
18 Southeast Asia, primarily because of the absence of internal mixing and
19 underestimated emissions. They recommended scaling up modeled BC AAOD to
20 AERONET observations in order to accurately estimate BC radiative effects.

21 Therefore, although surface BC concentration is relatively well captured by model
22 results (see Sect. 3.1), more measurements of vertical profiles over the Tibetan
23 Plateau are imperative for evaluating column quantities such as BC AAOD.

24 **4. Sensitivity to BC emissions**

25 Fig. 2 shows that model simulated surface BC concentrations are considerably lower
26 in Experiment B (using the INTEX-B inventory) relative to Experiment A (using the
27 LU inventory) at rural sites. The difference in surface BC concentration is more than
28 30% at rural sites and 10-20% at remote sites, decreasing with distance from the
29 source region. Such varying difference in surface BC concentration largely reflects
30 the spatially non-uniform differences between the two emission inventories. The
31 difference in BC concentration in snow between the two sets of results is less than

1 20%. The relatively smaller difference is because the sites with measurements of BC
2 concentration in snow are invariably remote high-elevation sites, further away from
3 the source regions. BC concentrations in snow are higher over the northwestern and
4 northeastern Plateau and to the north of the Plateau but lower in the Himalayas and
5 the central Plateau in Experiment B than in A. This is because of the lower BC
6 emissions in the central Plateau and India and the higher emissions in northwestern
7 and central China in the INTEX-B than in the LU inventories. BC AAOD values are
8 higher (< 15%) to the northeast and northwest of the Plateau and lower (10-60%) in
9 the Indo-Gangetic Plain in Experiment B than in A. Therefore, both surface BC
10 concentration and AAOD along the southern slope of the Himalayas are strongly
11 sensitive to Indian emissions, while the high-altitude remote sites are less affected by
12 the emission changes in the source regions. Overall, Experiment B results show larger
13 negative bias and root mean square error (RMSE) (Table 6) and lower Taylor score
14 (Fig. 10) relative to Experiment A. As such, our results suggest that the INTEX-B
15 inventory considerably underestimates anthropogenic BC emissions in India, which is
16 also implied by some latest estimates of BC emissions in Asia (Kurokawa et al., 2013;
17 Wang et al., 2014).

18 **5. Sensitivity to BC aging parameterization**

19 Compared with model results from the standard simulation (Experiment A, Table 5),
20 the use of Liu et al. (2011) parameterization for BC aging in the model (Experiment C,
21 Table 5) results in increased surface BC concentrations, BC concentrations in snow,
22 and BC AAOD, because of the longer BC atmospheric lifetime against wet
23 scavenging (see Sect. 2.2.3). The increase in surface BC concentration is 1% on
24 average (maximum 3%) at rural sites and 10% on average (maximum 30%) at remote
25 sites (Fig. 2). This is consistent with the results from Huang et al. (2013), where the
26 use of Liu et al. (2011) parameterization only changes GEOS-Chem simulated surface
27 BC concentrations by less than $0.01 \mu\text{g m}^{-3}$ in the Tibetan Plateau. Liu et al. (2011)
28 showed that their aging parameterization significantly improves seasonal variations of
29 modeled surface BC concentrations in the Arctic. This is different from the present
30 study, where the aging parameterization has a minor impact on the seasonality of both
31 surface BC concentrations and AAOD (Fig. 2 and Table 6). The increase in BC
32 AAOD is 10% on average (maximum 30%) at most AERONET sites but leads to

1 lower spatiotemporal correlations with observations (Table 6). The aging
2 parameterization has a much stronger impact on modeled BC concentration in snow
3 than on surface BC concentration and BC AAOD. The increase in BC concentration
4 in snow is more than 30% at a number of sites in the Himalayas and the central
5 Plateau (Table 2). Compared with the standard simulation (Experiment A), the use of
6 the Liu et al. (2011) parameterization results in an overestimate of BC concentration
7 in snow relative to observations, which increases the absolute bias by a factor of two
8 (Table 6) and decreases the Taylor score (Fig. 10). This suggests that the Liu et al.
9 (2011) aging parameterization may result in too long conversion times of BC (from
10 hydrophobic to hydrophilic) hence too long atmospheric lifetimes.

11 **6. Sensitivity to model resolution**

12 Compared with model results from the standard simulation (Experiment A, Table 5),
13 the use of a finer model resolution ($0.5^{\circ} \times 0.667^{\circ}$) nested over Asia (Experiment D,
14 Table 5) reduces the bias in modeled surface BC concentrations from 15% to 2% but
15 increases the RMSE (Table 6). Wang et al. (2014) found that replacing a coarse-
16 resolution model ($1.27^{\circ} \times 2.5^{\circ}$) with a finer-resolution one ($0.51^{\circ} \times 0.66^{\circ}$) reduces the
17 bias of surface BC simulation in Asia by 30%. Fig 2 shows that the nested model
18 simulation slightly improves seasonal variations of surface BC concentrations at
19 several remote sites, whereas it does not improve those at urban sites both in
20 magnitude and in temporal variation (Fig. 3). This is similar to the results in Fu et al.
21 (2012), where the GEOS-Chem nested model underestimates surface BC
22 concentrations by an order of magnitude at Dunhuang and Lhasa sites, even using the
23 enhanced BC emissions from top-down estimates. Compared with the standard
24 simulation, the nested model simulation increases the absolute bias by 57% in
25 modeled snow BC concentration and by 5% in modeled BC AAOD (Table 6). The
26 nested model results also show a lower spatiotemporal correlation with observations
27 of snow BC concentration and BC AAOD (Fig. 10). Our results suggest that the finer
28 model resolution alone cannot explain model versus observation discrepancies on the
29 simulation of snow BC concentration and BC AAOD in the Tibetan Plateau.

30 **7. Summary and conclusions**

31 This study sought to understand the capability of GEOS-Chem in simulating BC over
32 the Tibetan Plateau and the potential factors driving model versus observation

1 discrepancies. We used GEOS-Chem version 9-01-03 driven by GEOS-5 assimilated
2 meteorological fields and systematically evaluated the model simulations against *in*
3 *situ* measurements of BC in surface air, BC in snow, and BC AAOD for 2006. We
4 also examined the effects of anthropogenic BC emissions from China and India, BC
5 aging process and model resolution on BC simulations.

6 Model results captured the seasonal variation of surface BC concentrations at rural
7 sites, but the observed wintertime high values were absent in the model, which calls
8 for improved emission estimates particularly in the Indo-Gangetic Plain. The use of
9 non-local PBL mixing scheme reduced part of the discrepancy between observed and
10 modeled surface BC concentrations in winter. Modeled surface BC concentrations at
11 remote sites were within a factor of two of the observations. Part of the discrepancy is
12 explained by the inherent difficulty in simulating the meteorological fields over the
13 complex Himalayan terrain. Surface BC concentrations at urban sites are significantly
14 underestimated by model results.

15 Modeled BC concentrations in snow were spatiotemporally consistent with
16 observations ($r = 0.85$). The highest snow BC concentrations were seen north of the
17 Plateau (40°N-50°N), while the lowest values were found in the northern slope of the
18 Himalayas. However, model results were a factor of 2-4 higher than the observations
19 at three Himalayan sites during the monsoon, primarily because of the excessive BC
20 deposition resulted from overlong BC lifetime. Model results underestimated snow
21 BC concentration by a factor of two in the central Plateau, due to the lack of snow
22 aging in the CTM and the strong local emissions unaccounted for in the emission
23 inventories. Model results are consistent with the observations at the elevated sites in
24 the northwestern and northeastern Plateau and to the north of the Plateau. Model
25 results of both BC in snow and in surface air showed no statistically significant
26 difference with observations with biases less than 15%.

27 Modeled BC AAOD is consistently biased low at most AERONET sites over the
28 Plateau, especially to the northwest of the Plateau and in the Himalayas in winter and
29 spring. The large model versus observation discrepancies were mainly because of
30 underestimated emissions and the assumption of external mixing of BC in the model.
31 This suggests that modeled BC AAOD should be scaled to AERONET observations
32 in order to accurately estimate BC climatic effects. More measurements of vertical

1 profiles over the Tibetan Plateau are imperative for evaluating modeled column
2 quantities such as BC AAOD.

3 Sensitivity simulations showed that both surface BC concentration and BC AAOD
4 along the southern slope of the Himalayas were strongly sensitive to Indian emissions,
5 while the elevated remote sites were less affected by the change of emissions in
6 source regions. The BC aging parameterization from Liu et al. (2011) resulted in a
7 large increase of BC concentration in snow, but only had a minor impact on surface
8 BC concentration and AAOD. The use of a finer model resolution nested over Asia
9 reduced the bias in modeled surface BC concentration from 15% to 2%, but increased
10 the bias in modeled snow BC concentration and BC AAOD by 57% and 5%,
11 respectively. More quantitative analyses are required to investigate the uncertainties
12 in different model processes of BC simulations.

13 Therefore, accurate model simulations of BC in surface air, BC in snow and BC
14 AAOD over the Tibetan Plateau require improvements in BC emission inventories
15 particularly for China and India, model meteorological fields over the complex
16 Himalayan terrain, PBL mixing scheme particularly under a stable PBL condition,
17 model representation of atmospheric BC aging process including the conversion of
18 hydrophobic to hydrophilic BC and the enhancement of BC absorption resulted from
19 internal mixing, model parameterization of BC wet scavenging, and model simulation
20 of snow processes such as snow aging, snow melting and BC transfer among different
21 snow layers.

22

23 **Acknowledgements**

24 We thank three reviewers for their constructive comments. We thank Paolo Bonasoni,
25 Angela Marinoni, Stefano Decesari, Krishnaswamy Krishnamoorthy, Suresh Babu,
26 and Monika Kopacz for offering useful information. We thank James T. Randerson
27 for providing biomass burning emissions with small fires. K. Ram thanks Department
28 of Science and Technology, Govt. of India for providing financial support under the
29 INSPIRE Faculty scheme (No. DST/INSPIRE Faculty Award/2012; IFA-AES-02).
30 This study also used the data collected within the SHARE Project thanks to
31 contributions from the Italian National Research Council and the Italian Ministry of

1 Foreign Affairs. This study was funded by NASA grants NNX09AF07G and
2 NNX08AF64G from the Atmospheric Chemistry Modeling and Analysis Program
3 (ACMAP).

4

5 **References**

6 Akagi, S. K., Craven, J. S., Taylor, J. W., McMeeking, G. R., Yokelson, R. J., Burling,
7 I. R., Urbanski, S. P., Wold, C. E., Seinfeld, J. H., Coe, H., Alvarado, M. J., and
8 Weise, D. R.: Evolution of trace gases and particles emitted by a chaparral fire in
9 California, *Atmos. Chem. Phys.*, 12, 1397-1421, doi:10.5194/acp-12-1397-2012, 2012.

10 Allen, D. J., Rood, R. B., Thompson, A. M., and Hudson, R. D.: Three-dimensional
11 radon 222 calculations using assimilated meteorological data and a convective mixing
12 algorithm, *J. Geophys. Res.-Atmos.*, 101, 6871-6881, doi:10.1029/95jd03408, 1996a.

13 Allen, D. J., Kasibhatla, P., Thompson, A. M., Rood, R. B., Doddridge, B. G.,
14 Pickering, K. E., Hudson, R. D., and Lin, S. J.: Transport-induced interannual
15 variability of carbon monoxide determined using a chemistry and transport model, *J.*
16 *Geophys. Res.-Atmos.*, 101, 28655-28669, doi:10.1029/96jd02984, 1996b.

17 Andermann, C., Bonnet, S., and Gloaguen, R.: Evaluation of precipitation data sets
18 along the Himalayan front, *Geochem. Geophys. Geosy.*, 12, Q07023,
19 doi:10.1029/2011gc003513, 2011.

20 Arakawa, A., and Schubert, W. H.: Interaction of a Cumulus Cloud Ensemble with
21 Large-Scale Environment .1., *J. Atmos. Sci.*, 31, 674-701, doi:10.1175/1520-
22 0469(1974)031<0674:IOACCE>2.0.CO;2, 1974.

23 Barnett, T. P., Adam, J. C., and Lettenmaier, D. P.: Potential impacts of a warming
24 climate on water availability in snow-dominated regions, *Nature*, 438, 303-309,
25 doi:10.1038/Nature04141, 2005.

26 Beegum, S. N., Moorthy, K. K., Babu, S. S., Satheesh, S. K., Vinoj, V., Badarinath, K.
27 V. S., Safai, P. D., Devara, P. C. S., Singh, S., Vinod, Durnka, U. C., and Pant, P.:
28 Spatial distribution of aerosol black carbon over India during pre-monsoon season,
29 *Atmos. Environ.*, 43, 1071-1078, doi:10.1016/j.atmosenv.2008.11.042, 2009.

30 Bey, I., Jacob, D. J., Yantosca, R. M., Logan, J. A., Field, B. D., Fiore, A. M., Li, Q.
31 B., Liu, H. G. Y., Mickley, L. J., and Schultz, M. G.: Global modeling of tropospheric

1 chemistry with assimilated meteorology: Model description and evaluation, *J.
2 Geophys. Res.*, 106, 23073-23095, doi:10.1029/2001jd000807, 2001.

3 Bonasoni, P., Laj, P., Marinoni, A., Sprenger, M., Angelini, F., Arduini, J., Bonafe, U.,
4 Calzolari, F., Colombo, T., Decesari, S., Di Biagio, C., di Sarra, A. G., Evangelisti, F.,
5 Duchi, R., Facchini, M. C., Fuzzi, S., Gobbi, G. P., Maione, M., Panday, A., Roccato,
6 F., Sellegrini, K., Venzac, H., Verza, G. P., Villani, P., Vuillermoz, E., and Cristofanelli,
7 P.: Atmospheric Brown Clouds in the Himalayas: first two years of continuous
8 observations at the Nepal Climate Observatory-Pyramid (5079 m), *Atmos. Chem.
9 Phys.*, 10, 7515-7531, doi:10.5194/acp-10-7515-2010, 2010.

10 Bond, T. C., Anderson, T. L., and Campbell, D.: Calibration and intercomparison of
11 filter-based measurements of visible light absorption by aerosols, *Aerosol Sci. Tech.*,
12 30, 582-600, doi:10.1080/027868299304435, 1999.

13 Bond, T. C., Streets, D. G., Yarber, K. F., Nelson, S. M., Woo, J. H., and Klimont, Z.:
14 A technology-based global inventory of black and organic carbon emissions from
15 combustion, *J. Geophys. Res.*, 109, D14203, doi:10.1029/2003jd003697, 2004.

16 Bond, T. C., and Bergstrom, R. W.: Light absorption by carbonaceous particles: An
17 investigative review, *Aerosol Sci. Tech.*, 40, 27-67, doi:10.1080/02786820500421521,
18 2006.

19 Bond, T. C., Habib, G., and Bergstrom, R. W.: Limitations in the enhancement of
20 visible light absorption due to mixing state, *J. Geophys. Res.-Atmos.*, 111, D20211,
21 doi:10.1029/2006jd007315, 2006.

22 Bond, T. C., Bhardwaj, E., Dong, R., Jogani, R., Jung, S. K., Roden, C., Streets, D. G.,
23 and Trautmann, N. M.: Historical emissions of black and organic carbon aerosol from
24 energy-related combustion, 1850-2000, *Global Biogeochem. Cy.*, 21, Gb2018,
25 doi:10.1029/2006gb002840, 2007.

26 Bond, T. C., Doherty, S. J., Fahey, D. W., Forster, P. M., Berntsen, T., DeAngelo, B.
27 J., Flanner, M. G., Ghan, S., Kärcher, B., Koch, D., Kinne, S., Kondo, Y., Quinn, P.
28 K., Sarofim, M. C., Schultz, M. G., Schulz, M., Venkataraman, C., Zhang, H., Zhang,
29 S., Bellouin, N., Guttikunda, S. K., Hopke, P. K., Jacobson, M. Z., Kaiser, J. W.,
30 Klimont, Z., Lohmann, U., Schwarz, J. P., Shindell, D., Storelvmo, T., Warren, S. G.,
31 and Zender, C. S.: Bounding the role of black carbon in the climate system: A

1 scientific assessment, *J. Geophys. Res.-Atmos.*, 118, 1-173, doi:10.1002/jgrd.50171,
2 2013.

3 Cachier, H. and Pertuisot, M. H.: Particulate carbon in Arctic ice, *Analysis Magazine*,
4 22, 34–37, 1994.

5 Carrico, C. M., Bergin, M. H., Shrestha, A. B., Dibb, J. E., Gomes, L., and Harris, J.
6 M.: The importance of carbon and mineral dust to seasonal aerosol properties in the
7 Nepal Himalaya, *Atmos. Environ.*, 37, 2811-2824, doi:10.1016/S1352-
8 2310(03)00197-3, 2003.

9 Cappa, C. D., Onasch, T. B., Massoli, P., Worsnop, D. R., Bates, T. S., Cross, E. S.,
10 Davidovits, P., Hakala, J., Hayden, K. L., Jobson, B. T., Kolesar, K. R., Lack, D. A.,
11 Lerner, B. M., Li, S. M., Mellon, D., Nuaaman, I., Olfert, J. S., Petaja, T., Quinn, P.
12 K., Song, C., Subramanian, R., Williams, E. J., and Zaveri, R. A.: Radiative
13 Absorption Enhancements Due to the Mixing State of Atmospheric Black Carbon,
14 *Science*, 337, 1078-1081, doi:10.1126/science.1223447, 2012.

15 Chen, D., Wang, Y., McElroy, M. B., He, K., Yantosca, R. M., and Le Sager, P.:
16 Regional CO pollution and export in China simulated by the high-resolution nested-
17 grid GEOS-Chem model, *Atmos. Chem. Phys.*, 9, 3825-3839, 2009.

18 Chow, J. C., Watson, J. G., Chen, L. W. A., Arnott, W. P., Moosmuller, H., and Fung,
19 K.: Equivalence of elemental carbon by thermal/optical reflectance and transmittance
20 with different temperature protocols, *Environ. Sci. Technol.*, 38, 4414-4422,
21 doi:10.1021/Es034936u, 2004.

22 Clarke, A. D., Shinozuka, Y., Kapustin, V. N., Howell, S., Huebert, B., Doherty, S.,
23 Anderson, T., Covert, D., Anderson, J., Hua, X., Moore, K. G., McNaughton, C.,
24 Carmichael, G., and Weber, R.: Size distributions and mixtures of dust and black
25 carbon aerosol in Asian outflow: Physiochemistry and optical properties, *J. Geophys.*
26 *Res.-Atmos.*, 109, D15S09, doi:10.1029/2003jd004378, 2004.

27 Cooke, W. F., Lioussse, C., Cachier, H., and Feichter, J.: Construction of a 1 degrees x
28 1 degrees fossil fuel emission data set for carbonaceous aerosol and implementation
29 and radiative impact in the ECHAM4 model, *J. Geophys. Res.-Atmos.*, 104, 22137-
30 22162, doi:10.1029/1999jd900187, 1999.

1 Donner, L. J., Wyman, B. L., Hemler, R. S., Horowitz, L. W., Ming, Y., Zhao, M.,
2 Golaz, J. C., Ginoux, P., Lin, S. J., Schwarzkopf, M. D., Austin, J., Alaka, G., Cooke,
3 W. F., Delworth, T. L., Freidenreich, S. M., Gordon, C. T., Griffies, S. M., Held, I. M.,
4 Hurlin, W. J., Klein, S. A., Knutson, T. R., Langenhorst, A. R., Lee, H. C., Lin, Y. L.,
5 Magi, B. I., Malyshev, S. L., Milly, P. C. D., Naik, V., Nath, M. J., Pincus, R.,
6 Ploshay, J. J., Ramaswamy, V., Seman, C. J., Shevliakova, E., Sirutis, J. J., Stern, W.
7 F., Stouffer, R. J., Wilson, R. J., Winton, M., Wittenberg, A. T., and Zeng, F. R.: The
8 Dynamical Core, Physical Parameterizations, and Basic Simulation Characteristics of
9 the Atmospheric Component AM3 of the GFDL Global Coupled Model CM3, *J.
10 Climate*, 24, 3484-3519, doi:10.1175/2011jcli3955.1, 2011.

11 Dubovik, O., and King, M. D.: A flexible inversion algorithm for retrieval of aerosol
12 optical properties from Sun and sky radiance measurements, *J. Geophys. Res.-Atmos.*,
13 105, 20673-20696, doi:10.1029/2000jd900282, 2000.

14 Emery, C., Jung, J., Downey, N., Johnson, J., Jimenez, M., Yarvwood, G., and Morris,
15 R.: Regional and global modeling estimates of policy relevant background ozone over
16 the United States, *Atmos. Environ.*, 47, 206-217, doi:10.1016/j.atmosenv.2011.11.012,
17 2012.

18 Fairlie, T. D., Jacob, D. J., and Park, R. J.: The impact of transpacific transport of
19 mineral dust in the United States, *Atmos. Environ.*, 41, 1251-1266,
20 doi:10.1016/j.atmosenv.2006.09.048, 2007.

21 Flanner, M. G., Zender, C. S., Randerson, J. T., and Rasch, P. J.: Present-day climate
22 forcing and response from black carbon in snow, *J. Geophys. Res.-Atmos.*, 112,
23 D11202, doi:10.1029/2006jd008003, 2007.

24 Flanner, M. G., Zender, C. S., Hess, P. G., Mahowald, N. M., Painter, T. H.,
25 Ramanathan, V., and Rasch, P. J.: Springtime warming and reduced snow cover from
26 carbonaceous particles, *Atmos. Chem. Phys.*, 9, 2481-2497, 2009.

27 Friedman, B., Herich, H., Kammermann, L., Gross, D. S., Arneth, A., Holst, T., and
28 Cziczo, D. J.: Subarctic atmospheric aerosol composition: 1. Ambient aerosol
29 characterization, *J. Geophys. Res.-Atmos.*, 114, D13203, doi:10.1029/2009jd011772,
30 2009.

31 Fu, T. M., Cao, J. J., Zhang, X. Y., Lee, S. C., Zhang, Q., Han, Y. M., Qu, W. J., Han,
32 Z., Zhang, R., Wang, Y. X., Chen, D., and Henze, D. K.: Carbonaceous aerosols in

1 China: top-down constraints on primary sources and estimation of secondary
2 contribution, *Atmos. Chem. Phys.*, 12, 2725-2746, doi:10.5194/acp-12-2725-2012,
3 2012.

4 Ganguly, D., Ginoux, P., Ramaswamy, V., Dubovik, O., Welton, J., Reid, E. A., and
5 Holben, B. N.: Inferring the composition and concentration of aerosols by combining
6 AERONET and MPLNET data: Comparison with other measurements and utilization
7 to evaluate GCM output, *J. Geophys. Res.-Atmos.*, 114, D16203,
8 doi:10.1029/2009jd011895, 2009a.

9 Ganguly, D., Ginoux, P., Ramaswamy, V., Winker, D. M., Holben, B. N., and
10 Tripathi, S. N.: Retrieving the composition and concentration of aerosols over the
11 Indo-Gangetic basin using CALIOP and AERONET data, *Geophys. Res. Lett.*, 36,
12 L13806, doi:10.1029/2009gl038315, 2009b.

13 Granier, C., Bessagnet, B., Bond, T., D'Angiola, A., van der Gon, H. D., Frost, G. J.,
14 Heil, A., Kaiser, J. W., Kinne, S., Klimont, Z., Kloster, S., Lamarque, J. F., Liousse,
15 C., Masui, T., Meleux, F., Mieville, A., Ohara, T., Raut, J. C., Riahi, K., Schultz, M.
16 G., Smith, S. J., Thompson, A., van Aardenne, J., van der Werf, G. R., and van
17 Vuuren, D. P.: Evolution of anthropogenic and biomass burning emissions of air
18 pollutants at global and regional scales during the 1980-2010 period, *Climatic Change*,
19 109, 163-190, doi:10.1007/s10584-011-0154-1, 2011.

20 Hack, J. J.: Parameterization of moist convection in the National Center for
21 Atmospheric Research community climate model (CCM2), *J. Geophys. Res.-Atmos.*,
22 99, 5551-5568, doi:10.1029/93jd03478, 1994.

23 Hansen, J., and Nazarenko, L.: Soot climate forcing via snow and ice albedos, *P. Natl.*
24 *Acad. Sci. USA*, 101, 423-428, doi:10.1073/pnas.2237157100, 2004.

25 Harris, I., Jones, P. D., Osborn, T. J., and Lister, D. H.: Updated high-resolution grids
26 of monthly climatic observations – the CRU TS3.10 Dataset, *Int. J. Climatol.*, 34,
27 623-642, doi:10.1002/joc.3711, 2014.

28 Holtslag, A. A. M., and Boville, B. A.: Local Versus Nonlocal Boundary-Layer
29 Diffusion in a Global Climate Model, *J. Climate*, 6, 1825-1842, doi:10.1175/1520-
30 0442(1993)006<1825:Lvnbl>2.0.Co;2, 1993.

1 Huang, Y., Wu, S., Dubey, M. K., and French, N. H. F.: Impact of aging mechanism
2 on model simulated carbonaceous aerosols, *Atmos. Chem. Phys.*, 13, 6329-6343,
3 doi:10.5194/acp-13-6329-2013, 2013.

4 Huffman, G. J., Adler, R. F., Morrissey, M. M., Bolvin, D. T., Curtis, S., Joyce, R.,
5 McGavock, B., and Susskind, J.: Global precipitation at one-degree daily resolution
6 from multisatellite observations, *J. Hydrometeorol.*, 2, 36-50, doi:10.1175/1525-
7 7541(2001)002<0036:Gpaodd>2.0.Co;2, 2001.

8 Immerzeel, W. W., van Beek, L. P. H., and Bierkens, M. F. P.: Climate Change Will
9 Affect the Asian Water Towers, *Science*, 328, 1382-1385,
10 doi:10.1126/science.1183188, 2010.

11 Jacobson, M. Z.: Strong radiative heating due to the mixing state of black carbon in
12 atmospheric aerosols, *Nature*, 409, 695-697, doi:10.1038/35055518, 2001.

13 Jacobson, M. Z.: Climate response of fossil fuel and biofuel soot, accounting for
14 soot's feedback to snow and sea ice albedo and emissivity, *J. Geophys. Res.-Atmos.*,
15 109, D21201, doi:10.1029/2004jd004945, 2004.

16 Jacobson, M. Z.: Effects of externally-through-internally-mixed soot inclusions within
17 clouds and precipitation on global climate, *J. Phys. Chem. A.*, 110, 6860-6873,
18 doi:10.1021/Jp056391r, 2006.

19 Kaiser, J. W., Heil, A., Andreae, M. O., Benedetti, A., Chubarova, N., Jones, L.,
20 Morcrette, J. J., Razinger, M., Schultz, M. G., Suttie, M., and van der Werf, G. R.:
21 Biomass burning emissions estimated with a global fire assimilation system based on
22 observed fire radiative power, *Biogeosciences*, 9, 527-554, doi:10.5194/bg-9-527-
23 2012, 2012.

24 Khalizov, A. F., Zhang, R. Y., Zhang, D., Xue, H. X., Pagels, J., and McMurry, P. H.:
25 Formation of highly hygroscopic soot aerosols upon internal mixing with sulfuric acid
26 vapor, *J. Geophys. Res.-Atmos.*, 114, D05208, doi:10.1029/2008jd010595, 2009.

27 Kitoh, A., and Kusunoki, S.: East Asian summer monsoon simulation by a 20-km
28 mesh AGCM, *Clim. Dynam.*, 31, 389-401, doi:10.1007/s00382-007-0285-2, 2008.

29 Koch, D., Schulz, M., Kinne, S., McNaughton, C., Spackman, J. R., Balkanski, Y.,
30 Bauer, S., Berntsen, T., Bond, T. C., Boucher, O., Chin, M., Clarke, A., De Luca, N.,
31 Dentener, F., Diehl, T., Dubovik, O., Easter, R., Fahey, D. W., Feichter, J., Fillmore,

1 D., Freitag, S., Ghan, S., Ginoux, P., Gong, S., Horowitz, L., Iversen, T., Kirkevag, A.,
2 Klimont, Z., Kondo, Y., Krol, M., Liu, X., Miller, R., Montanaro, V., Moteki, N.,
3 Myhre, G., Penner, J. E., Perlitz, J., Pitari, G., Reddy, S., Sahu, L., Sakamoto, H.,
4 Schuster, G., Schwarz, J. P., Seland, O., Stier, P., Takegawa, N., Takemura, T., Textor,
5 C., van Aardenne, J. A., and Zhao, Y.: Evaluation of black carbon estimations in
6 global aerosol models, *Atmos. Chem. Phys.*, 9, 9001-9026, 2009.

7 Kopacz, M., Mauzerall, D. L., Wang, J., Leibensperger, E. M., Henze, D. K., and
8 Singh, K.: Origin and radiative forcing of black carbon transported to the Himalayas
9 and Tibetan Plateau, *Atmos. Chem. Phys.*, 11, 2837-2852, doi:10.5194/acp-11-2837-
10 2011, 2011.

11 Kurokawa, J., Ohara, T., Morikawa, T., Hanayama, S., Janssens-Maenhout, G., Fukui,
12 T., Kawashima, K., and Akimoto, H.: Emissions of air pollutants and greenhouse
13 gases over Asian regions during 2000-2008: Regional Emission inventory in ASia
14 (REAS) version 2, *Atmos. Chem. Phys.*, 13, 11019-11058, doi:10.5194/acp-13-
15 11019-2013, 2013.

16 Lamarque, J. F., Bond, T. C., Eyring, V., Granier, C., Heil, A., Klimont, Z., Lee, D.,
17 Liousse, C., Mieville, A., Owen, B., Schultz, M. G., Shindell, D., Smith, S. J.,
18 Stehfest, E., Van Aardenne, J., Cooper, O. R., Kainuma, M., Mahowald, N.,
19 McConnell, J. R., Naik, V., Riahi, K., and van Vuuren, D. P.: Historical (1850-2000)
20 gridded anthropogenic and biomass burning emissions of reactive gases and aerosols:
21 methodology and application, *Atmos. Chem. Phys.*, 10, 7017-7039, doi:10.5194/acp-
22 10-7017-2010, 2010.

23 Lau, K. M., and Kim, K. M.: Observational relationships between aerosol and Asian
24 monsoon rainfall, and circulation, *Geophys. Res. Lett.*, 33, L21810,
25 doi:10.1029/2006gl027546, 2006.

26 Lau, W. K. M., Kim, M. K., Kim, K. M., and Lee, W. S.: Enhanced surface warming
27 and accelerated snow melt in the Himalayas and Tibetan Plateau induced by
28 absorbing aerosols, *Environ. Res. Lett.*, 5, 025204, doi:10.1088/1748-
29 9326/5/2/025204, 2010.

30 Lin, J. T., Youn, D., Liang, X. Z., and Wuebbles, D. J.: Global model simulation of
31 summertime US ozone diurnal cycle and its sensitivity to PBL mixing, spatial

1 resolution, and emissions, *Atmos. Environ.*, 42, 8470-8483,
2 doi:10.1016/j.atmosenv.2008.08.012, 2008.

3 Lin, J. T., and McElroy, M. B.: Impacts of boundary layer mixing on pollutant
4 vertical profiles in the lower troposphere: Implications to satellite remote sensing,
5 *Atmos. Environ.*, 44, 1726-1739, doi:10.1016/j.atmosenv.2010.02.009, 2010.

6 Lin, S. J., and Rood, R. B.: Multidimensional flux-form semi-Lagrangian transport
7 schemes, *Mon. Weather Rev.*, 124, 2046-2070, doi:10.1175/1520-
8 0493(1996)124<2046:MFFSLT>2.0.CO;2, 1996.

9 Liu, H. Y., Jacob, D. J., Bey, I., and Yantosca, R. M.: Constraints from Pb-210 and
10 Be-7 on wet deposition and transport in a global three-dimensional chemical tracer
11 model driven by assimilated meteorological fields, *J. Geophys. Res.-Atmos.*, 106,
12 12109-12128, doi:10.1029/2000jd900839, 2001.

13 Liu, J. F., Fan, S. M., Horowitz, L. W., and Levy, H.: Evaluation of factors
14 controlling long-range transport of black carbon to the Arctic, *J. Geophys. Res.-*
15 *Atmos.*, 116, D04307, doi:10.1029/2010jd015145, 2011.

16 Louis, J. F.: Parametric Model of Vertical Eddy Fluxes in the Atmosphere, Bound-
17 Lay. *Meteorol.*, 17, 187-202, doi:10.1007/Bf00117978, 1979.

18 Lu, Z., Zhang, Q., and Streets, D. G.: Sulfur dioxide and primary carbonaceous
19 aerosol emissions in China and India, 1996-2010, *Atmos. Chem. Phys.*, 11, 9839-
20 9864, doi:10.5194/acp-11-9839-2011, 2011.

21 Lu, Z. F., Streets, D. G., Zhang, Q., and Wang, S. W.: A novel back-trajectory
22 analysis of the origin of black carbon transported to the Himalayas and Tibetan
23 Plateau during 1996-2010, *Geophys. Res. Lett.*, 39, L01809,
24 doi:10.1029/2011gl049903, 2012.

25 Ma, L. J., Zhang, T., Frauenfeld, O. W., Ye, B. S., Yang, D. Q., and Qin, D. H.:
26 Evaluation of precipitation from the ERA-40, NCEP-1, and NCEP-2 Reanalyses and
27 CMAP-1, CMAP-2, and GPCP-2 with ground-based measurements in China, *J.*
28 *Geophys. Res.-Atmos.*, 114, D09105, doi:10.1029/2008jd011178, 2009.

29 Marks, D., Link, T., Winstral, A., and Garen, D.: Simulating snowmelt processes
30 during rain-on-snow over a semi-arid mountain basin, *Annals of Glaciology*, 32, 195-
31 202, doi:10.3189/172756401781819751, 2001.

1 Mao, Y. H., Li, Q. B., Zhang, L., Chen, Y., Randerson, J. T., Chen, D., and Liou, K.
2 N.: Biomass burning contribution to black carbon in the Western United States
3 Mountain Ranges, *Atmos. Chem. Phys.*, 11, 11253-11266, doi:10.5194/acp-11-
4 11253-2011, 2011.

5 McMeeking, G. R., Good, N., Petters, M. D., McFiggans, G., and Coe, H.: Influences
6 on the fraction of hydrophobic and hydrophilic black carbon in the atmosphere,
7 *Atmos. Chem. Phys.*, 11, 5099-5112, doi:10.5194/acp-11-5099-2011, 2011.

8 Ménégoz, M., Gallée, H., and Jacobi, H.-W., Precipitation and snow cover in the
9 Himalaya: From reanalysis to regional climate simulations, *Hydrol. Earth Syst. Sci.*,
10 17, 3921-3936, doi:10.5194/hess-17-3921-2013, 2013. Menon, S., Koch, D., Beig, G.,
11 Sahu, S., Fasullo, J., and Orlikowski, D.: Black carbon aerosols and the third polar ice
12 cap, *Atmos. Chem. Phys.*, 10, 4559-4571, doi:10.5194/acp-10-4559-2010, 2010.

13 Mikhailov, E. F., Vlasenko, S. S., Kramer, L., and Niessner, R.: Interaction of soot
14 aerosol particles with water droplets: influence of surface hydrophilicity, *J. Aerosol*
15 *Sci.*, 32, 697-711, doi:10.1016/S0021-8502(00)00101-4, 2001.

16 Ming, J., Cachier, H., Xiao, C., Qin, D., Kang, S., Hou, S., and Xu, J.: Black carbon
17 record based on a shallow Himalayan ice core and its climatic implications, *Atmos.*
18 *Chem. Phys.*, 8, 1343-1352, 2008.

19 Ming, J., Xiao, C. D., Cachier, H., Qin, D. H., Qin, X., Li, Z. Q., and Pu, J. C.: Black
20 Carbon (BC) in the snow of glaciers in west China and its potential effects on albedos,
21 *Atmos. Res.*, 92, 114-123, doi:10.1016/j.atmosres.2008.09.007, 2009a.

22 Ming, J., Xiao, C., Du, Z., and Flanner, M. G.: Black carbon in snow/ice of west
23 China and its radiative forcing, *Adv. Climate Change Res.*, 5(6), 328–35, 2009b (in
24 Chinese with English abstract).

25 Ming, J., Xiao, C. D., Sun, J. Y., Kang, S. C., and Bonasoni, P.: Carbonaceous
26 particles in the atmosphere and precipitation of the Nam Co region, central Tibet, *J.*
27 *Environ. Sci.-China*, 22, 1748-1756, doi:10.1016/S1001-0742(09)60315-6, 2010.

28 Ming, J., Du, Z. C., Xiao, C. D., Xu, X. B., and Zhang, D. Q.: Darkening of the mid-
29 Himalaya glaciers since 2000 and the potential causes, *Environ. Res. Lett.*, 7, 014021,
30 doi:10.1088/1748-9326/7/1/014021, 2012.

1 Ming, J., Xiao, C. D., Du, Z. C., and Yang, X. G.: An overview of black carbon
2 deposition in High Asia glaciers and its impacts on radiation balance, *Advances in*
3 *Water Resources*, 55, 80-87, doi:10.1016/j.advwatres.2012.05.015, 2013.

4 Moorthi, S., and Suarez, M. J.: Relaxed Arakawa-Schubert - a Parameterization of
5 Moist Convection for General-Circulation Models, *Mon. Weather Rev.*, 120, 978-
6 1002, doi:10.1175/1520-0493(1992)120<0978:Rasapo>2.0.Co;2, 1992.

7 Moorthy, K. K., Beegum, S. N., Srivastava, N., Satheesh, S. K., Chin, M., Blond, N.,
8 Babu, S. S., and Singh, S.: Performance evaluation of chemistry transport models over
9 India, *Atmos. Environ.*, 71, 210-225, 2013.

10 Nair, V. S., Moorthy, K. K., Alappattu, D. P., Kunhikrishnan, P. K., George, S., Nair,
11 P. R., Babu, S. S., Abish, B., Satheesh, S. K., Tripathi, S. N., Niranjan, K., Madhavan,
12 B. L., Srikant, V., Dutt, C. B. S., Badarinath, K. V. S., and Reddy, R. R.: Wintertime
13 aerosol characteristics over the Indo-Gangetic Plain (IGP): Impacts of local boundary
14 layer processes and long-range transport, *J. Geophys. Res.-Atmos.*, 112, D13205,
15 doi:10.1029/2006jd008099, 2007.

16 Nair, V. S., Solmon, F., Giorgi, F., Mariotti, L., Babu, S. S., and Moorthy, K. K.:
17 Simulation of South Asian aerosols for regional climate studies, *J. Geophys. Res.-*
18 *Atmos.*, 117, D04209, doi:10.1029/2011JD016711, 2012.

19 Painter, T. H., Flanner, M. G., Kaser, G., Marzeion, B., VanCuren, R. A., and
20 Abdalati, W.: End of the Little Ice Age in the Alps forced by industrial black carbon,
21 *P. Natl. Acad. Sci. USA*, 110, 15216-15221, doi:10.1073/pnas.1302570110, 2013.

22 Park, R. J., Jacob, D. J., Chin, M., and Martin, R. V.: Sources of carbonaceous
23 aerosols over the United States and implications for natural visibility, *J. Geophys.*
24 *Res.-Atmos.*, 108, 4355, doi:10.1029/2002jd003190, 2003.

25 Park, R. J., Jacob, D. J., Palmer, P. I., Clarke, A. D., Weber, R. J., Zondlo, M. A.,
26 Eisele, F. L., Bandy, A. R., Thornton, D. C., Sachse, G. W., and Bond, T. C.: Export
27 efficiency of black carbon aerosol in continental outflow: Global implications, *J.*
28 *Geophys. Res.-Atmos.*, 110, D11205, doi:10.1029/2004jd005432, 2005.

29 Park, R. J., Jacob, D. J., Kumar, N., and Yantosca, R. M.: Regional visibility statistics
30 in the United States: Natural and transboundary pollution influences, and implications

1 for the Regional Haze Rule, *Atmos. Environ.*, 40, 5405-5423,
2 doi:10.1016/j.atmosenv.2006.04.059, 2006.

3 Pathak, B., Kalita, G., Bhuyan, K., Bhuyan, P. K., and Moorthy, K. K.: Aerosol
4 temporal characteristics and its impact on shortwave radiative forcing at a location in
5 the northeast of India, *J. Geophys. Res.-Atmos.*, 115, D19204,
6 doi:10.1029/2009jd013462, 2010.

7 Petzold, A., and Schonlinner, M.: Multi-angle absorption photometry - a new method
8 for the measurement of aerosol light absorption and atmospheric black carbon, *J.*
9 *Aerosol Sci.*, 35, 421-441, doi:10.1016/j.jaerosci.2003.09.005, 2004.

10 Poschl, U., Letzel, T., Schauer, C., and Niessner, R.: Interaction of ozone and water
11 vapor with spark discharge soot aerosol particles coated with benzo[a]pyrene: O₃ and
12 H₂O adsorption, benzo[a]pyrene degradation, and atmospheric implications, *J. Phys.*
13 *Chem. A.*, 105, 4029-4041, doi:10.1021/Jp004137n, 2001.

14 Prasad, A. K., Yang, K. H. S., El-Askary, H. M., and Kafatos, M.: Melting of major
15 Glaciers in the western Himalayas: evidence of climatic changes from long term MSU
16 derived tropospheric temperature trend (1979-2008), *Ann. Geophys.-Germany*, 27,
17 4505-4519, 2009.

18 Qian, Y., Flanner, M. G., Leung, L. R., and Wang, W.: Sensitivity studies on the
19 impacts of Tibetan Plateau snowpack pollution on the Asian hydrological cycle and
20 monsoon climate, *Atmos. Chem. Phys.*, 11, 1929-1948, doi:10.5194/acp-11-1929-
21 2011, 2011.

22 Qin, D. H., Liu, S. Y., and Li, P. J.: Snow cover distribution, variability, and response
23 to climate change in western China, *J. Climate*, 19, 1820-1833, 2006.

24 Qin, Y., and Xie, S. D.: Spatial and temporal variation of anthropogenic black carbon
25 emissions in China for the period 1980-2009, *Atmos. Chem. Phys.*, 12, 4825-4841,
26 doi:10.5194/acp-12-4825-2012, 2012.

27 Qu, W. J., Zhang, X. Y., Arimoto, R., Wang, D., Wang, Y. Q., Yan, L. W., and Li, Y.:
28 Chemical composition of the background aerosol at two sites in southwestern and
29 northwestern China: potential influences of regional transport, *Tellus B.*, 60, 657-673,
30 doi:10.1111/j.1600-0889.2008.00342.x, 2008.

1 Ram, K., Sarin, M. M., and Hegde, P.: Long-term record of aerosol optical properties
2 and chemical composition from a high-altitude site (Manora Peak) in Central
3 Himalaya, *Atmos. Chem. Phys.*, 10, 11791-11803, doi:10.5194/acp-10-11791-2010,
4 2010a.

5 Ram, K., Sarin, M. M., and Tripathi, S. N.: A 1 year record of carbonaceous aerosols
6 from an urban site in the Indo-Gangetic Plain: Characterization, sources, and temporal
7 variability, *J. Geophys. Res.-Atmos.*, 115, D24313, doi:10.1029/2010jd014188,
8 2010b.

9 Ramanathan, V., Chung, C., Kim, D., Bettge, T., Buja, L., Kiehl, J. T., Washington,
10 W. M., Fu, Q., Sikka, D. R., and Wild, M.: Atmospheric brown clouds: Impacts on
11 South Asian climate and hydrological cycle, *P. Natl. Acad. Sci. USA*, 102, 5326-5333,
12 doi:10.1073/pnas.0500656102, 2005.

13 Ramanathan, V., Ramana, M. V., Roberts, G., Kim, D., Corrigan, C., Chung, C., and
14 Winker, D.: Warming trends in Asia amplified by brown cloud solar absorption,
15 *Nature*, 448, 575-578, doi:10.1038/Nature06019, 2007.

16 Ramanathan, V., and Carmichael, G.: Global and regional climate changes due to
17 black carbon, *Nat. Geosci.*, 1, 221-227, doi:10.1038/Ngeo156, 2008.

18 Randerson, J. T., Chen, Y., van der Werf, G. R., Rogers, B. M., and Morton, D. C.:
19 Global burned area and biomass burning emissions from small fires, *J. Geophys. Res.-*
20 *Biogeosci.*, 117, G04012, doi:10.1029/2012jg002128, 2012.

21 Sato, M., Hansen, J., Koch, D., Lacis, A., Ruedy, R., Dubovik, O., Holben, B., Chin,
22 M., and Novakov, T.: Global atmospheric black carbon inferred from AERONET, P.
23 *Natl. Acad. Sci. USA*, 100, 6319-6324, doi:10.1073/pnas.0731897100, 2003.

24 Schmid, H., Laskus, L., Abraham, H. J., Baltensperger, U., Lavanchy, V., Bizjak, M.,
25 Burba, P., Cachier, H., Crow, D., Chow, J., Gnauk, T., Even, A., ten Brink, H. M.,
26 Giesen, K. P., Hitzenberger, R., Hueglin, C., Maenhaut, W., Pio, C., Carvalho, A.,
27 Putaud, J. P., Toom-Sauntry, D., and Puxbaum, H.: Results of the "carbon
28 conference" international aerosol carbon round robin test stage I, *Atmos. Environ.*, 35,
29 2111-2121, doi:10.1016/S1352-2310(00)00493-3, 2001.

30 Seinfeld, J. H., and S. N. Pandis, *Atmospheric Chemistry and Physics, From Air
31 Pollution to Climate Change*, 2nd ed., John Wiley, Hoboken, N. J, 490-530, 2006.

1 Singh, H. B., Brune, W. H., Crawford, J. H., Flocke, F., and Jacob, D. J.: Chemistry
2 and transport of pollution over the Gulf of Mexico and the Pacific: spring 2006
3 INTEX-B campaign overview and first results, *Atmos. Chem. Phys.*, 9, 2301-2318,
4 2009.

5 Streets, D. G., Bond, T. C., Carmichael, G. R., Fernandes, S. D., Fu, Q., He, D.,
6 Klimont, Z., Nelson, S. M., Tsai, N. Y., Wang, M. Q., Woo, J. H., and Yarber, K. F.:
7 An inventory of gaseous and primary aerosol emissions in Asia in the year 2000, *J.
8 Geophys. Res.-Atmos.*, 108, 8809, doi:10.1029/2002jd003093, 2003.

9 Taylor, K. E.: Summarizing multiple aspects of model performance in a single
10 diagram, *J. Geophys. Res.-Atmos.*, 106, 7183-7192, doi:10.1029/2000jd900719, 2001.

11 Textor, C., Schulz, M., Guibert, S., Kinne, S., Balkanski, Y., Bauer, S., Berntsen, T.,
12 Berglen, T., Boucher, O., Chin, M., Dentener, F., Diehl, T., Easter, R., Feichter, H.,
13 Fillmore, D., Ghan, S., Ginoux, P., Gong, S., Kristjansson, J. E., Krol, M., Lauer, A.,
14 Lamarque, J. F., Liu, X., Montanaro, V., Myhre, G., Penner, J., Pitari, G., Reddy, S.,
15 Seland, O., Stier, P., Takemura, T., and Tie, X.: Analysis and quantification of the
16 diversities of aerosol life cycles within AeroCom, *Atmos. Chem. Phys.*, 6, 1777-1813,
17 2006.

18 van der Werf, G. R., Randerson, J. T., Giglio, L., Collatz, G. J., Mu, M., Kasibhatla, P.
19 S., Morton, D. C., DeFries, R. S., Jin, Y., and van Leeuwen, T. T.: Global fire
20 emissions and the contribution of deforestation, savanna, forest, agricultural, and peat
21 fires (1997-2009), *Atmos. Chem. Phys.*, 10, 11707-11735, doi:10.5194/acp-10-11707-
22 2010, 2010.

23 Voisin, N., Wood, A. W., and Lettenmaier, D. P.: Evaluation of precipitation products
24 for global hydrological prediction, *J. Hydrometeorol.*, 9, 388-407,
25 doi:10.1175/2007jhm938.1, 2008.

26 Walcek, C. J., Brost, R. A., Chang, J. S., and Wesely, M. L.: So₂, Sulfate and H_{NO}₃
27 Deposition Velocities Computed Using Regional Land-Use and Meteorological Data,
28 *Atmos. Environ.*, 20, 949-964, doi:10.1016/0004-6981(86)90279-9, 1986.

29 Wang, Q., Jacob, D. J., Fisher, J. A., Mao, J., Leibensperger, E. M., Carouge, C. C.,
30 Le Sager, P., Kondo, Y., Jimenez, J. L., Cubison, M. J., and Doherty, S. J.: Sources of
31 carbonaceous aerosols and deposited black carbon in the Arctic in winter-spring:

1 implications for radiative forcing, *Atmos. Chem. Phys.*, 11, 12453-12473,
2 doi:10.5194/acp-11-12453-2011, 2011.

3 Wang, Q., Jacob, D. J., Spackman, J. R., Perring, A. E., Schwarz, J. P., Moteki, N.,
4 Marais, E. A., Ge, C., Wang, J., and Barrett, S. R. H.: Global budget and radiative
5 forcing of black carbon aerosol: Constraints from pole-to-pole (HIPPO) observations
6 across the Pacific, *J. Geophys. Res.-Atmos.*, 119, 195-206,
7 doi:10.1002/2013jd020824, 2014.

8 Wang, R., Tao, S., Wang, W. T., Liu, J. F., Shen, H. Z., Shen, G. F., Wang, B., Liu, X.
9 P., Li, W., Huang, Y., Zhang, Y. Y., Lu, Y., Chen, H., Chen, Y. C., Wang, C., Zhu, D.,
10 Wang, X. L., Li, B. G., Liu, W. X., and Ma, J. M.: Black Carbon Emissions in China
11 from 1949 to 2050, *Environ. Sci. Technol.*, 46, 7595-7603, doi:10.1021/Es3003684,
12 2012.

13 Wang, R., Tao, S., Balkanski, Y., Ciais, P., Boucher, O., Liu, J. F., Piao, S. L., Shen,
14 H. Z., Vuolo, M. R., Valari, M., Chen, H., Chen, Y. C., Cozic, A., Huang, Y., Li, B.
15 G., Li, W., Shen, G. F., Wang, B., and Zhang, Y. Y.: Exposure to ambient black
16 carbon derived from a unique inventory and high-resolution model, *P. Natl. Acad. Sci.
17 USA.*, 111, 2459-2463, doi:10.1073/pnas.1318763111, 2014.

18 Wang, Y. H., Jacob, D. J., and Logan, J. A.: Global simulation of tropospheric O₃-
19 NO_x-hydrocarbon chemistry 1. Model formulation, *J. Geophys. Res.-Atmos.*, 103,
20 10713-10725, doi:10.1029/98jd00158, 1998.

21 Weingartner, E., Saathoff, H., Schnaiter, M., Streit, N., Bitnar, B., and Baltensperger,
22 U.: Absorption of light by soot particles: determination of the absorption coefficient
23 by means of aethalometers, *J. Aerosol Sci.*, 34, 1445-1463, doi:10.1016/S0021-
24 8502(03)00359-8, 2003.

25 Wesely, M. L.: Parameterization of Surface Resistances to Gaseous Dry Deposition in
26 Regional-Scale Numerical Models, *Atmos. Environ.*, 23, 1293-1304,
27 doi:10.1016/0004-6981(89)90153-4, 1989.

28 Wu, Q. B., and Liu, Y. Z.: Ground temperature monitoring and its recent change in
29 Qinghai-Tibet Plateau, *Cold Reg. Sci. Technol.*, 38, 85-92, doi:10.1016/S0165-
30 232x(03)00064-8, 2004.

1 Xie, P. P., and Arkin, P. A.: Global precipitation: A 17-year monthly analysis based
2 on gauge observations, satellite estimates, and numerical model outputs, *B. Am.*
3 *Meteorol. Soc.*, 78, 2539-2558, doi:10.1175/1520-
4 0477(1997)078<2539:Gpagma>2.0.Co;2, 1997.

5 Xie, P. P., Yatagai, A., Chen, M. Y., Hayasaka, T., Fukushima, Y., Liu, C. M., and
6 Yang, S.: A Gauge-based analysis of daily precipitation over East Asia, *J.*
7 *Hydrometeorol.*, 8, 607-626, doi:10.1175/Jhm583.1, 2007.

8 Xu, B., Yao, T., Liu, X., and Wang, N.: Elemental and organic carbon measurements
9 with a two-step heating-gas chromatography system in snow samples from the
10 Tibetan plateau, *Ann. Glaciol.*, 43, 257–262, doi:10.3189/172756406781812122,
11 2006.

12 Xu, B. Q., Cao, J. J., Hansen, J., Yao, T. D., Joswia, D. R., Wang, N. L., Wu, G. J.,
13 Wang, M., Zhao, H. B., Yang, W., Liu, X. Q., and He, J. Q.: Black soot and the
14 survival of Tibetan glaciers, *P. Natl. Acad. Sci. USA*, 106, 22114-22118,
15 doi:10.1073/pnas.0910444106, 2009.

16 Yasunari, T. J., Bonasoni, P., Laj, P., Fujita, K., Vuillermoz, E., Marinoni, A.,
17 Cristofanelli, P., Duchi, R., Tartari, G., and Lau, K. M.: Estimated impact of black
18 carbon deposition during pre-monsoon season from Nepal Climate Observatory -
19 Pyramid data and snow albedo changes over Himalayan glaciers, *Atmos. Chem. Phys.*,
20 10, 6603-6615, doi:10.5194/acp-10-6603-2010, 2010.

21 Zhang, Q., Streets, D. G., Carmichael, G. R., He, K. B., Huo, H., Kannari, A.,
22 Klimont, Z., Park, I. S., Reddy, S., Fu, J. S., Chen, D., Duan, L., Lei, Y., Wang, L. T.,
23 and Yao, Z. L.: Asian emissions in 2006 for the NASA INTEX-B mission, *Atmos.*
24 *Chem. Phys.*, 9, 5131-5153, 2009.

25 Zhang, R. Y., Khalizov, A. F., Pagels, J., Zhang, D., Xue, H. X., and McMurry, P. H.:
26 Variability in morphology, hygroscopicity, and optical properties of soot aerosols
27 during atmospheric processing, *P. Natl. Acad. Sci. USA*, 105, 10291-10296,
28 doi:10.1073/pnas.0804860105, 2008.

29 Zhang, X. Y., Wang, Y. Q., Zhang, X. C., Guo, W., and Gong, S. L.: Carbonaceous
30 aerosol composition over various regions of China during 2006, *J. Geophys. Res.-*
31 *Atmos.*, 113, D14111, doi:10.1029/2007jd009525, 2008.

1 Zhao, T. B., and Fu, C. B.: Comparison of products from ERA-40, NCEP-2, and CRU
2 with station data for summer precipitation over China, *Adv. Atmos. Sci.*, 23, 593-604,
3 doi:10.1007/s00376-006-0593-1, 2006.

4 Zhou, G., Yao, T., Kang, S., Pu, J., Tian, L., Yang, W.: Mass balance of the Zhadang
5 glacier in the central Tibetan Plateau. *J. Glaciol. Geocryol.*, 29(3), 360-365, 2007 (in
6 Chinese with English abstract).

7

1 **Table 1.** Observed and simulated surface BC concentrations over the Tibetan Plateau
 2 (see also **Fig. 1**).

Region	Site	Lat. (°N)	Lon. (°E)	Elev. (m)	Time	Freq.	Technique ^a	Surface BC (μg m ⁻³)				
								Obs. ^b	Exp.A ^c	Exp.B ^d	Exp.C ^e	Exp. D ^f
Urban	Delhi	28.6	77.2	260	2006	monthly	Aethalometer	13.5 ^[1]	2.6 (1.6-4.7)	1.7	2.6	2.6
	Dibrugarh	27.3	94.6	111	2008-2009	monthly	Aethalometer	8.9 ^[2]	0.8 (0.5-1.5)	0.5	0.9	1.6
	Lhasa	29.7	91.1	3663	2006	monthly	TOR	3.7 ^[3]	0.08 (0.05-0.14)	0.07	0.09	0.05
	Dunhuang	40.2	94.7	1139	2006	monthly	TOR	4.1 ^[3]	0.1 (0.08-0.24)	0.2	0.1	0.3
Rural	Kharagpur	22.5	87.5	28	2006	monthly	Aethalometer	5.5 ^[4]	4.2 (2.5-8.4)	2.4	4.2	6.1
	Kanpur	26.4	80.3	142	2006	monthly	TOT	3.7 ^[5]	3.1 (1.0-5.8)	2.2	3.1	2.8
	Gandhi College	25.9	84.1	158	2006	monthly	Retrieval	4.8 ^[6]	4.6 (2.9-8.5)	3.2	4.6	5.0
Remote	Nagarkot	27.7	85.5	2150	1999-2000	seasonal	TOT	1.0 ^[7]	0.8 (0.5-1.3)	0.7	0.8	0.7
	NCOP	28.0	86.8	5079	2006	monthly	MAAP	0.2 ^[8]	0.07 (0.05-0.13)	0.07	0.08	0.07
	Manora Peak	29.4	79.5	1950	2006	monthly	TOT	1.1 ^[9]	1.3 (0.9-2.2)	1.2	1.3	1.2
	NCOS	30.8	91.0	4730	2006	monthly	TOR	0.1 ^[10]	0.08 (0.05-0.15)	0.07	0.09	0.04
	Langtang	28.1	85.6	3920	1999-2000	seasonal	TOT	0.4 ^[7]	0.4 (0.2-0.7)	0.4	0.4	0.5
	Zhuzhang	28.0	99.7	3583	2004-2005	monthly	TOR	0.3 ^[11]	0.3 (0.2-0.5)	0.3	0.4	0.3

3 ^aThermal Optical Reflectance (TOR), Thermal Optical Transmittance (TOT), Multi-Angle
 4 Absorption Photometer (MAAP)

5 ^bValues are multi-month averages. References: ^[1]Beegum et al. (2009), ^[2]Pathak et al. (2010),
 6 ^[3]Zhang et al. (2008), ^[4]Nair et al. (2012), ^[5]Ram et al. (2010b), ^[6]Ganguly et al. (2009b),
 7 ^[7]Carrico et al. (2003), ^[8]Bonasoni et al. (2010), ^[9]Ram et al. (2010a), ^[10]Ming et al. (2010),
 8 ^[11]Qu et al. (2008).

9 ^cValues from Experiment A (Table 5) for 2006. See text for details. Values in parentheses are
 10 from the same Experiment but using instead the upper and lower bounds of anthropogenic BC
 11 emissions in China and India.

12 ^dValues from Experiment B (Table 5) for 2006. See text for details.

13 ^eValues from Experiment C (Table 5) for 2006. See text for details.

14 ^fValues from Experiment D (Table 5) for 2006. See text for details.

15

16

17

1 **Table 2.** Observed and simulated BC concentrations in snow over the Tibetan Plateau
 2 (see also **Fig. 1**).

Region	Site	Lat. (°N)	Lon. (°E)	Elev. (km)	Time	BC in snow ($\mu\text{g kg}^{-1}$)				
						Obs. ^a	Exp.A ^b	Exp.B ^c	Exp.C ^d	Exp.D ^e
The Himalayas	Zuoqiupu	29.21	96.92	5.50	monsoon 2006	7.9 ^[2]	22.5 (13.6-43.0)	18.4	25.5	24.6
		29.21	96.92	5.60	non-monsoon 2006	15.9 ^[2]	21.2 (13.6-36.9)	18.3	31.9	53.9
	Qiangyong	28.83	90.25	5.40	summer 2001	43.1 ^[1]	66.1 (42.2-122.8)	49.7	63.7	18.3
	Noijin Kangsang	29.04	90.20	5.95	annual 2005	30.6 ^[2]	39.5 (21.1-60.8)	34.6	52.3	22.5
	East Rongbuk	28.02	86.96	6.50	monsoon 2001	35.0 ^[3]	26.4 (16.8-48.9)	22.7	29.2	22.4
		28.02	86.96	6.50	non-monsoon 2001	21.0 ^[3]	32.8 (21.6-55.6)	31.1	59.4	42.7
		28.02	86.96	6.50	summer 2002	20.3 ^[4]	26.5 (16.8-49.3)	22.8	28.9	23.0
		28.02	86.96	6.50	Oct. 2004	18.0 ^[4]	20.5 (13.6-35.6)	20.8	26.0	25.4
		28.02	86.96	6.50	Sept. 2006	9.0 ^[7]	26.0 (16.7-47.6)	22.4	30.0	20.6
	Kangwure	28.47	85.82	6.00	May 2007	41.8 ^[6]	27.1 (16.9-41.7)	24.7	29.7	45.2
	Namunani	30.45	81.27	5.90	summer 2001	21.8 ^[1]	26.5 (16.8-49.3)	22.8	28.9	18.0
	summer 2004	4.3 ^[1]	24.8 (15.8-45.2)	21.2	26.6	19.6				
Northwestern Tibetan Plateau	Mt. Muztagh	38.28	75.02	6.35	summer 2001	37.2 ^[1]	31.0 (23.3-52.8)	36.6	31.9	32.9
		38.28	75.10	6.30	1999	26.6 ^[1]	33.0 (26.6-48.6)	36.4	45.8	42.1
Northeastern Tibetan Plateau	Laohugou #12	39.43	96.56	5.05	Oct. 2005	35.0 ^[4]	54.4 (34.9-97.2)	60.0	60.3	65.0
	Qiyi	39.23	97.06	4.85	Jul. 2005	22.0 ^[4]	25.7 (18.5-67.0)	30.3	27.4	48.9
	July1 glacier	39.23	97.75	4.60	summer 2001	52.6 ^[1]	59.2 (32.8-122.8)	68.8	61.0	106.2
Central Tibetan Plateau	Meikuang	35.67	94.18	5.20	summer 2001	446 ^[1]	24.4 (15.4-47.0)	24.8	27.2	32.9
		35.67	94.18	5.20	Nov. 2005	81.0 ^[5]	40.9 (18.8-50.0)	43.3	50.5	38.6
	Tanggula	33.11	92.09	5.80	2003	53.1 ^[2]	16.1 (10.4-28.6)	14.5	25.6	12.0
	Dongkemadi	33.10	92.08	5.60	summer 2001	18.2 ^[1]	19.6 (12.2-36.8)	17.7	22.1	15.0
		33.10	92.08	5.60	year 2005	36.0 ^[7]	15.8 (10.2-28.1)	14.2	23.7	11.8
	La'nong	30.42	90.57	5.85	Jun. 2005	67.0 ^[4]	39.1 (25.8-72.9)	35.9	37.8	22.9
	Zhadang	30.47	90.50	5.80	Jul. 2006	87.4 ^[4]	27.9 (17.0-53.4)	21.7	30.3	19.3
North of the Plateau	Haxilegen River	43.73	84.46	3.76	Oct. 2006	46.9 ^[4]	36.1 (34.1-45.2)	37.9	36.7	71.4
		43.10	86.82	4.05	Nov. 2006	141 ^[5]	131.9 (71.8-270.4)	155.2	118.4	127.9
	Miao'ergou #3	43.06	94.32	4.51	Aug. 2005	111 ^[4]	98.8 (59.3-158.2)	113.2	103.7	113.8

3 ^aReferences: ^[1]Xu et al. (2006), ^[2]Xu et al. (2009), ^[3]Ming et al. (2008), ^[4]Ming et al. (2009a),
 4 ^[5]Ming et al. (2009b), ^[6]Ming et al. (2012), ^[7]Ming et al. (2013).

1 ^bValues from Experiment A (Table 5) for 2006. See text for details. Values in parentheses are
2 from the same Experiment but using instead the upper and lower bounds of anthropogenic BC
3 emissions in China and India.

4 ^cValues from Experiment B (Table 5) for 2006. See text for details.

5 ^dValues from Experiment C (Table 5) for 2006. See text for details.

6 ^eValues from Experiment D (Table 5) for 2006. See text for details.

7

8

1 **Table 3.** Observed and simulated annual mean BC AAOD at AERONET sites over
 2 the Tibetan Plateau (see also **Fig. 1**).

Region	Site	Lat. (°N)	Lon. (°E)	Alt. (m)	Time	BC AAOD		
						Obs. ^a	Model ^b	Ratio ^c
The Indo-Gangetic Plain	Lahore	31.54	74.33	270	2007~2012	0.0434	0.0162 (0.0125-0.0239)	2.7
	Kanpur	26.51	80.23	123	2006~2012	0.0426	0.0221 (0.0071-0.0413)	1.9
	Gandhi College	25.87	84.13	60	2006~2012	0.0443	0.0282 (0.0179-0.0517)	1.6
	Gual_Pahari	28.43	77.15	384	2008~2010	0.0511	0.0222 (0.0147-0.0382)	2.3
	Jaipur	26.91	75.81	450	2009~2012	0.0202	0.0168 (0.0110-0.0296)	1.2
The Himalayas	Jomsom	28.78	83.71	2803	2012	0.0231	0.0136 (0.0092-0.0228)	1.7
	Pantnagar	29.05	79.52	241	2008~2009	0.0507	0.0114 (0.0079-0.0193)	4.4
	Nainital	29.36	79.46	1939	2008~2010	0.0204	0.0125 (0.0086-0.0212)	1.6
	Pokhara	28.15	83.97	807	2010~2012	0.0524	0.0056 (0.0037-0.0097)	9.4
	Kathmandu Univ.	27.60	85.54	1510	2009~2010	0.0406	0.0057 (0.0038-0.0099)	7.1
Northeastern Tibetan Plateau	SACOL	35.95	104.14	1965	2007~2011	0.0163	0.0100 (0.0056-0.0204)	1.6
Northeast of the Tibetan Plateau	Dalanzadgad	43.58	104.42	1470	2006, 2012	0.0038	0.0025 (0.0020-0.0041)	1.5
Northwest of the Tibetan Plateau	Issyk-Kul	42.62	76.98	1650	2008~2010	0.0196	0.0020 (0.0017-0.0029)	9.8
	Dushanbe	38.55	68.86	821	2011~2012	0.0131	0.0030 (0.0027-0.0035)	4.4

3 ^aAERONET retrieved BC AAOD (Bond et al., 2013). Values are multi-year averages.

4 ^bValues from Experiment A (Table 5) for 2006. See text for details. Values in parentheses are
 5 from the same Experiment but using instead the upper and lower bounds of anthropogenic BC
 6 emissions in China and India.

7 ^cThe ratio of AERONET retrieved to GEOS-Chem modeled BC AAOD.

8

9

10

1 **Table 4.** Anthropogenic BC emissions in China and India in 2006.

	China		India	
Emissions (Gg yr ⁻¹)	Lu et al. (2011)	Zhang et al. (2009)	Lu et al. (2011)	Zhang et al. (2009)
Industry	509	575	201	47
Power plants	15	36	1	8
Residential	971	1022	608	268
Transportation	178	205	75	80
Total	1673 (954-3229*)	1838 (884-3823)	885 (522-1655)	404 (112-1454)

*Uncertainties (in parentheses).

1 **Table 5.** GEOS-Chem simulations of BC.

Model experiment	A	B	C	D
Resolution	$2^\circ \times 2.5^\circ$	$2^\circ \times 2.5^\circ$	$2^\circ \times 2.5^\circ$	$0.5^\circ \times 0.667^\circ$ (Asia) $2^\circ \times 2.5^\circ$ (Global)
Anthropogenic emissions	China & India	Lu et al. (2011)	Zhang et al. (2009)	Lu et al. (2011)
	Rest of Asia		Zhang et al. (2009)	
	Rest of world		Bond et al. (2007)	
Biomass burning emissions	GFEDv3 (van der Werf et al., 2010), with updates from Randerson et al. (2012)			
BC aging (hydrophobic to hydrophilic)	e-folding time 1.15 days	e-folding time 1.15 days	Liu et al. (2011)	e-folding time 1.15 days
Deposition	Dry deposition	Wesely (1989) as implemented by Wang et al. (1998)		
	Wet deposition	Liu et al. (2001) with updates from Wang et al. (2011)		

2
3
4

1 **Table 6.** Error statistics of GEOS-Chem simulations of BC in the Tibetan Plateau for
 2 2006.

Statistical quantities [*]	BC in surface air				BC in snow				BC AAOD			
	Model experiments (see Table 5)											
	A	B	C	D	A	B	C	D	A	B	C	D
Mean Error	-0.29	-0.82	-0.26	-0.03	-1.23	-0.75	3.39	1.94	-0.019	-0.023	-0.020	-0.020
Mean Absolute Error	0.59	0.93	0.59	0.74	13.39	12.74	16.09	19.67	0.020	0.023	0.020	0.021
Fractional Gross Error	0.39	0.46	0.39	0.46	0.43	0.40	0.48	0.58	0.78	0.93	0.80	0.77
Root Mean Square Error (RMSE)	1.34	1.95	1.33	1.33	16.73	16.65	18.67	24.54	0.026	0.029	0.027	0.027
Bias-corrected RMSE	1.31	1.77	1.30	1.33	16.69	16.63	18.36	24.46	0.017	0.018	0.018	0.019
Correlation coefficient (<i>p</i> -value < 0.001)	0.90	0.87	0.90	0.87	0.85	0.86	0.81	0.70	0.53	0.46	0.45	0.37

3 *Units for mean error, mean absolute error, RMSE and bias-corrected RMSE are $\mu\text{g m}^{-3}$ for BC in
 4 surface air and $\mu\text{g kg}^{-1}$ for BC in snow.
 5

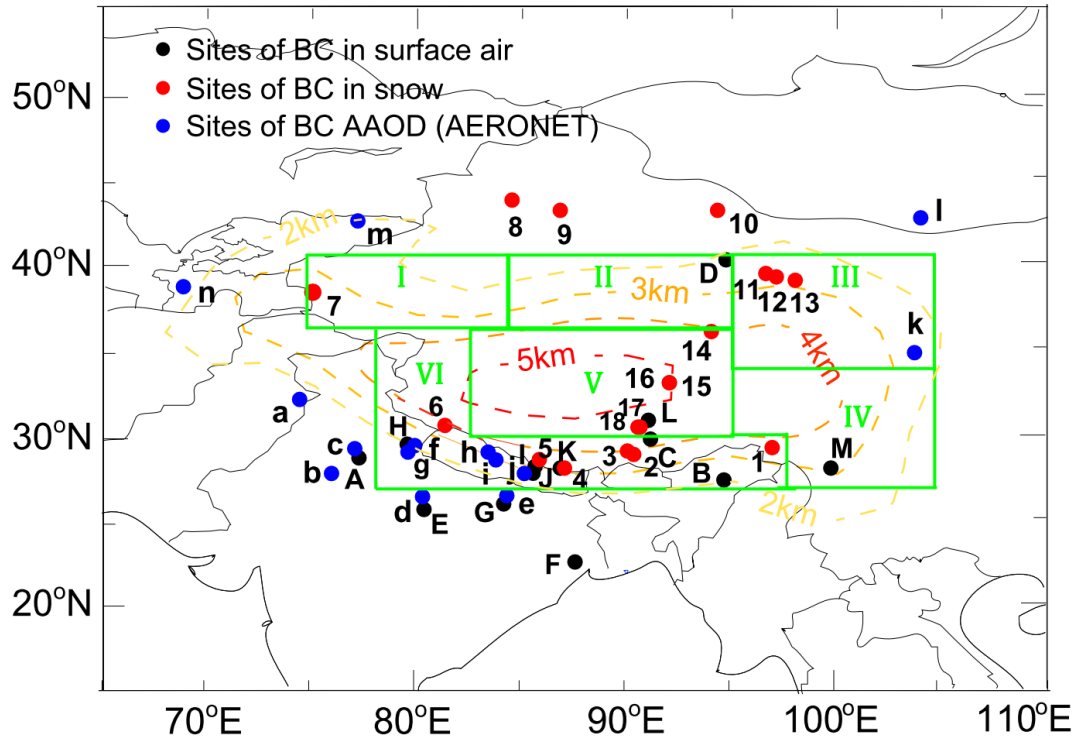


Fig. 1. BC measurements at sites in and around the Tibetan Plateau (see also Tables 1, 2 and 3). Black circles are surface measurements: Delhi (A), Dibragarh (B), Lhasa (C), Dunhuang (D), Kanpur (E), Kharagpur (F), Gandhi College (G), Manora Peak (H), Langtang (I), Nagarkot (J), Nepal Climate Observatory at Pyramid (NCOP, K), Nam Co Observational Station (NCOS, L), Zhuzhang (M). Red circles are measurements of BC in snow: Zuoqiupu (1), Qiangyong (2), Noijin Kangsang (3), East Rongbuk (4), Kangwure (5), Namunani (6), Mt. Muztagh (7), Haxilegen Riverhead (8), Urumqi Riverhead (9), Miao'ergou No.3 (10), Laozugou No. 12 (11), Qiyi (12), July 1 glacier (13), Meikuang (14), Tanggula (15), Dongkemadi (16), La'nong (17), Zhadang (18). Blue circles are BC AAOD measurements: Lahore (a), Jaipur (b), Gual_Pahari (c), Kanpur (d), Gandhi college (e), Nainital (f), Pantnagar (g), Jomsom (h), Pokhara (i), Kathmandu University (j), SACOL (k), Dalanzadgad (l), Issyk-Kul (m), Dushanbe (n). The rectangles are the six sub-regions: the northwestern Plateau (I), the northern Plateau (II), the northeastern Plateau (III), the southeastern Plateau (IV), the central Plateau (V), and the Himalayas (VI). Topography is also shown (dashed colored contours).

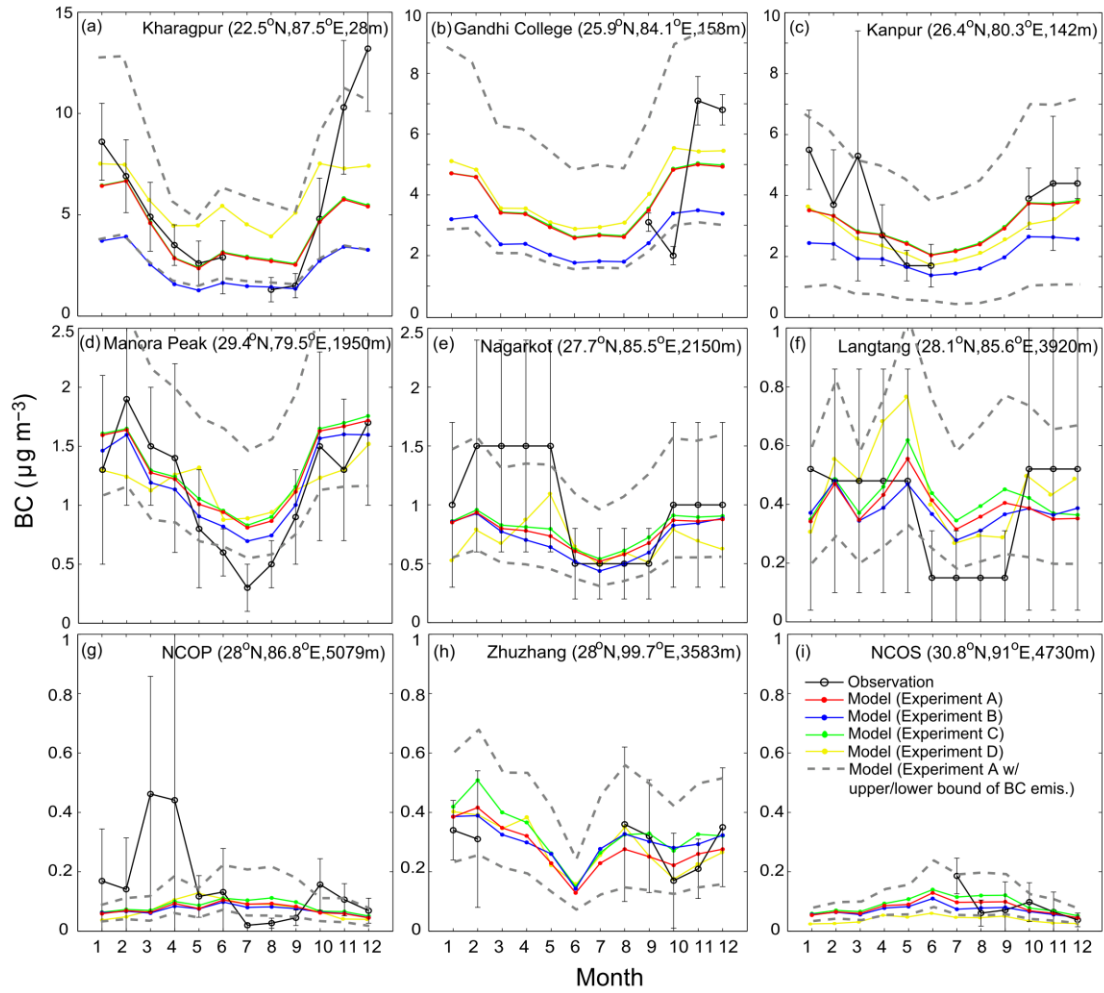


Fig. 2. Observed (black curve) and GEOS-Chem simulated (colored curves: red - Experiment A; blue - Experiment B; green - Experiment C; yellow - Experiment D; grey dashed curves - Experiment A using upper/lower bounds of anthropogenic BC emissions in China and India) monthly mean surface BC concentration ($\mu\text{g m}^{-3}$) at three rural sites (a-c) and six remote sites (d-i) over the Tibetan Plateau in 2006 (see Table 1 and Fig. 1). Only seasonal mean observations are available at sites e and f. Also shown are standard deviations for observations (error bars). See text for details.

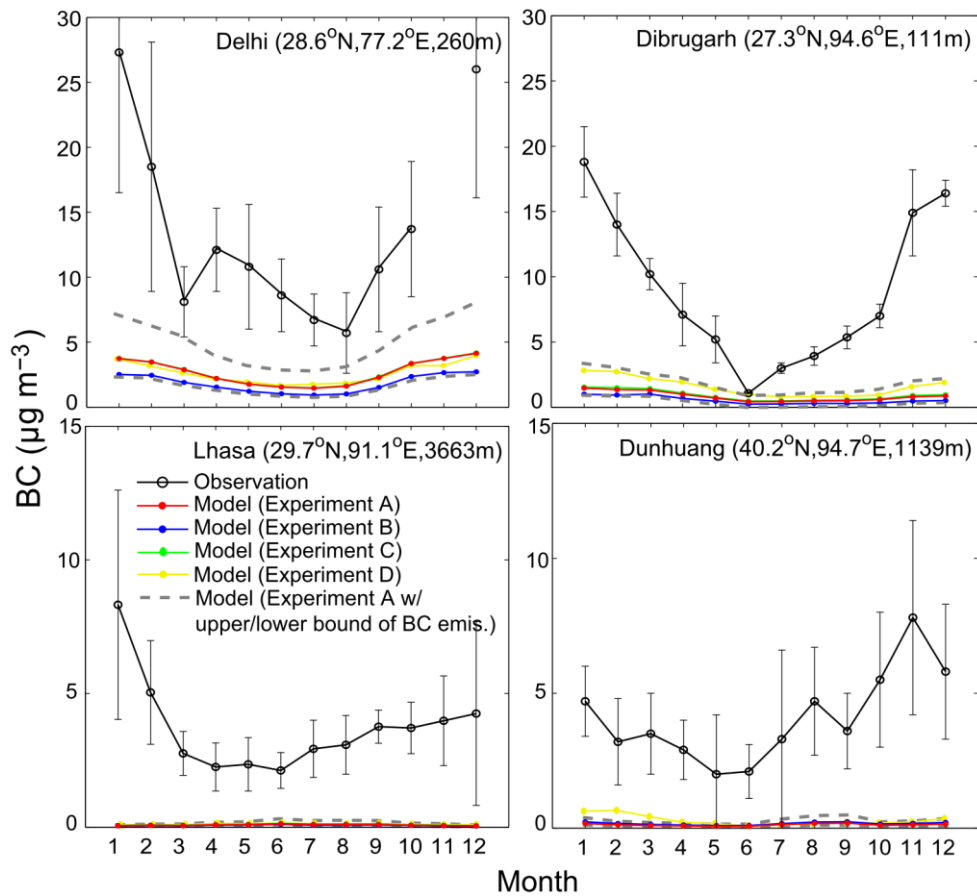


Fig. 3. Same as Fig. 2, but for four urban sites (see Table 1 and Fig. 1).

1
2
3
4

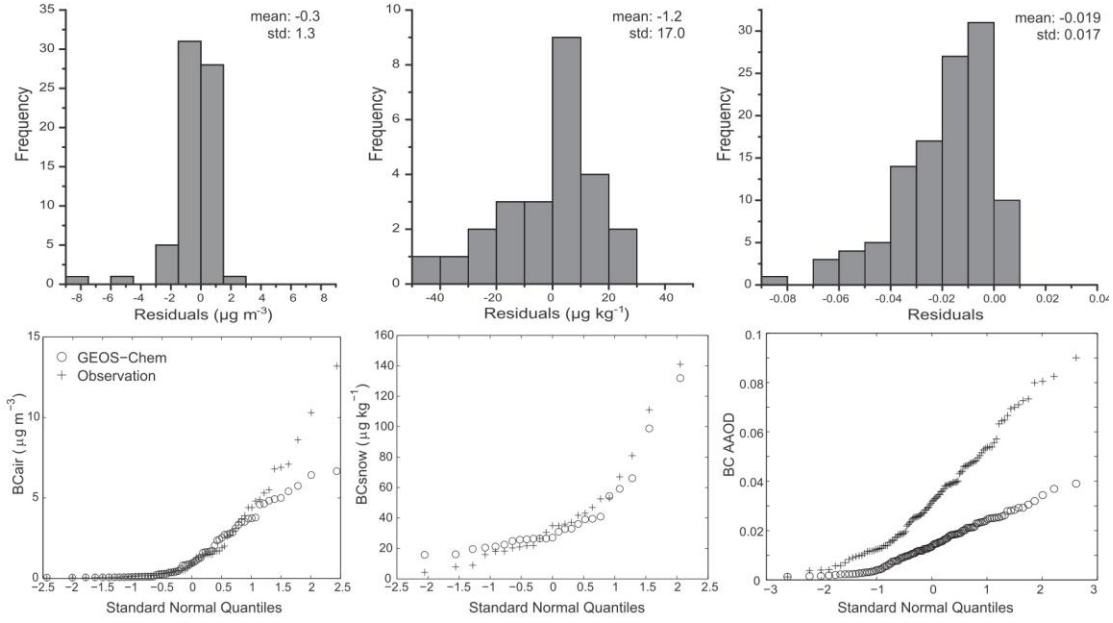
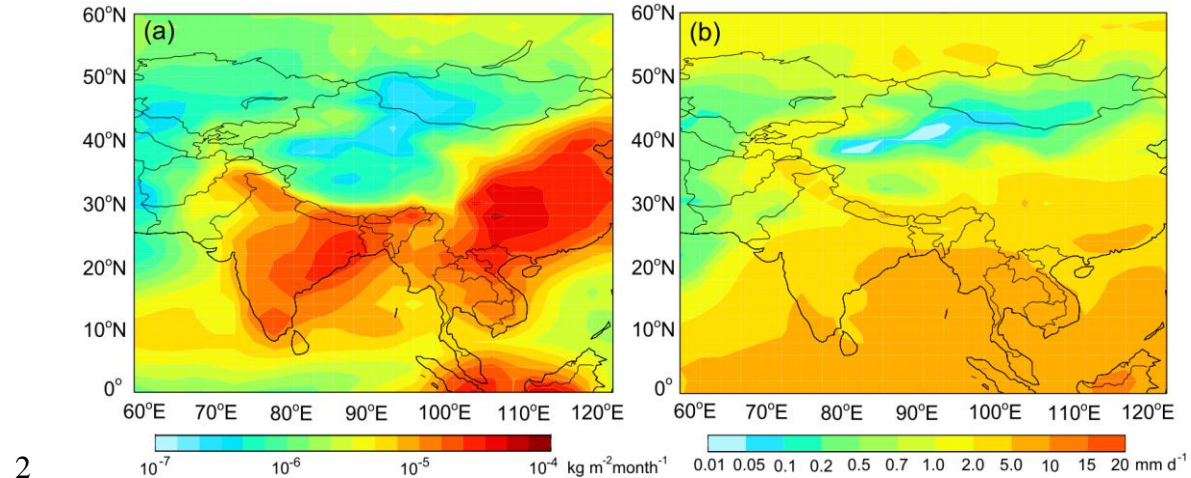


Fig. 4. Frequency histogram of residual errors (model - observation) (top row) and cumulative probability distributions (bottom row) for surface BC (left column), BC in snow (middle column), and BC AAOD (right column) at sites in and around the Tibetan Plateau (see Tables 1, 2 and 3 and Fig. 1). Also shown are the mean and standard deviation of residual errors. Values are for 2006 unless stated otherwise. See text for details.

1
2

9
10
11

1



2

4 **Fig. 5.** (a) GEOS-Chem simulated annual mean total BC deposition ($\text{kg m}^{-2} \text{month}^{-1}$)
5 over Asia and (b) GEOS-5 annual mean total precipitation (mm day^{-1}) over Asia.
6 Values are for 2006.

7

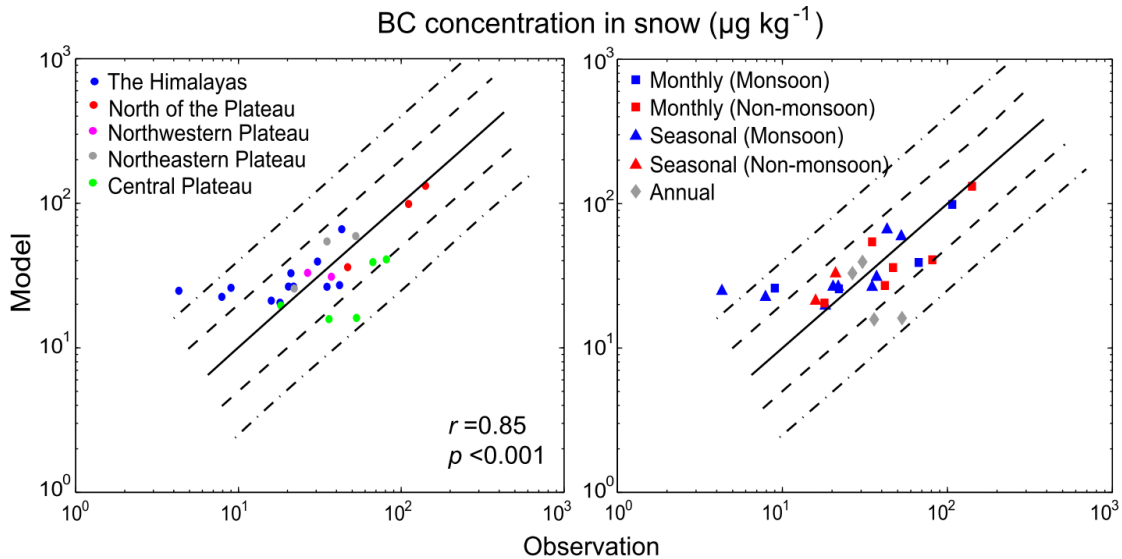
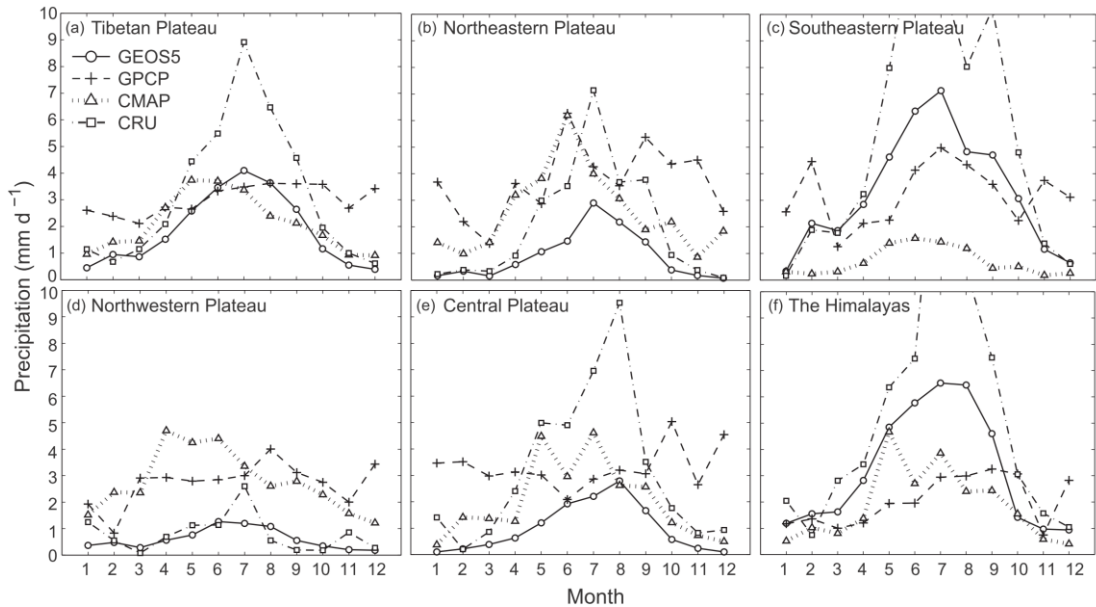


Fig. 6. Observed and GEOS-Chem simulated monthly or seasonal mean BC concentration in snow ($\mu\text{g kg}^{-1}$) at sites over the Tibetan Plateau (see Table 2 and Fig. 1). Left panel: sub-regions of the Tibetan Plateau are color-coded. Right panel: different temporal resolutions are symbol-coded: monthly - square; seasonal - triangle; annual - diamond, with blue for monsoon season and red for non-monsoon season. Solid lines are 1:1 ratio lines; dashed lines are 1:2 (or 2:1) ratio lines; dashed-dotted lines are 1:4 (or 4:1) ratio lines. Also shown are the correlation coefficient (r) and p -value. Values are for 2006 unless stated otherwise. See text for details.

1



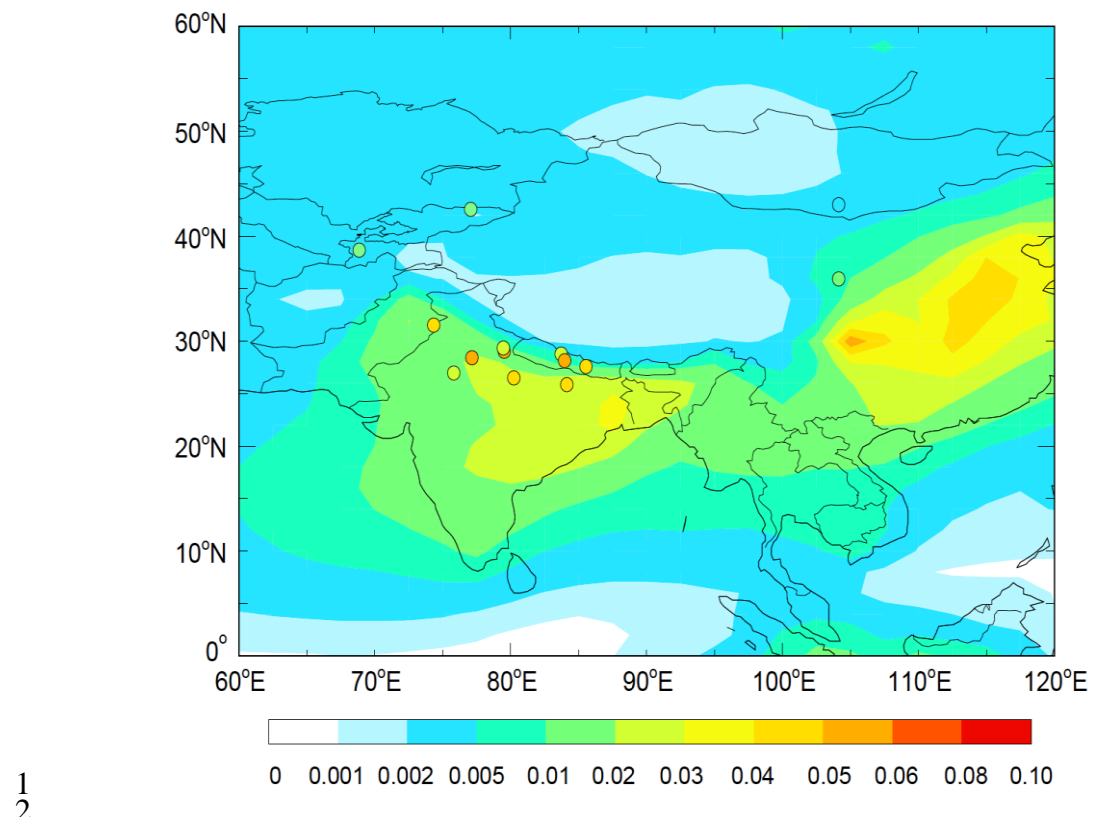
2

3

4 **Fig. 7.** Monthly mean precipitation (mm d^{-1}) in 2006, averaged over different parts of
 5 the Tibetan Plateau (see Fig. 1). Data is from the Goddard Earth Observing System
 6 Model version 5 data assimilation system (GEOS-5 DAS), Global Precipitation
 7 Climatology Project (GPCP), NOAA Climate Prediction Center (CPC) Merged
 8 Analysis of Precipitation (CMAP), and Climate Research Unit (CRU) of University of
 9 East Anglia.

10

11



1
2 **Fig. 8.** GEOS-Chem simulated annual mean BC AAOD (color contours) for 2006.
3 Colored circles are values retrieved from AERONET observations (see Table 3).
4
5
6
7

1

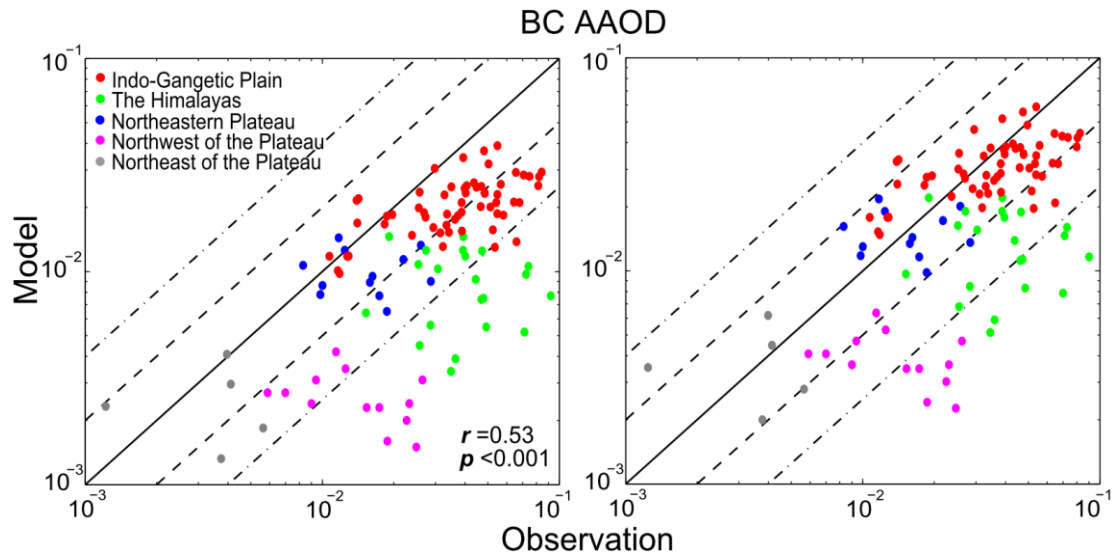


Fig. 9. Observed and GEOS-Chem simulated monthly mean BC AAOD at AERONET sites over the Tibetan Plateau (see Table 3 and Fig. 1). Left panel: assuming external mixing of BC. Right panel: assuming a 50% increase of BC absorption associated with internal mixing. Regions are color-coded: Indo-Gangetic Plain (red), the Himalayas (green), the northeastern Plateau (blue), Northeast of the Plateau (grey), Northwest of the Plateau (magenta). Solid line is 1:1 ratio line; dashed lines are 1:2 (or 2:1) ratio lines; dashed-dotted lines are 1:4 (or 4:1) ratio lines. Also shown are the correlation coefficient (r) and p -value. Values are for 2006 unless stated otherwise. See text for details.

13

1

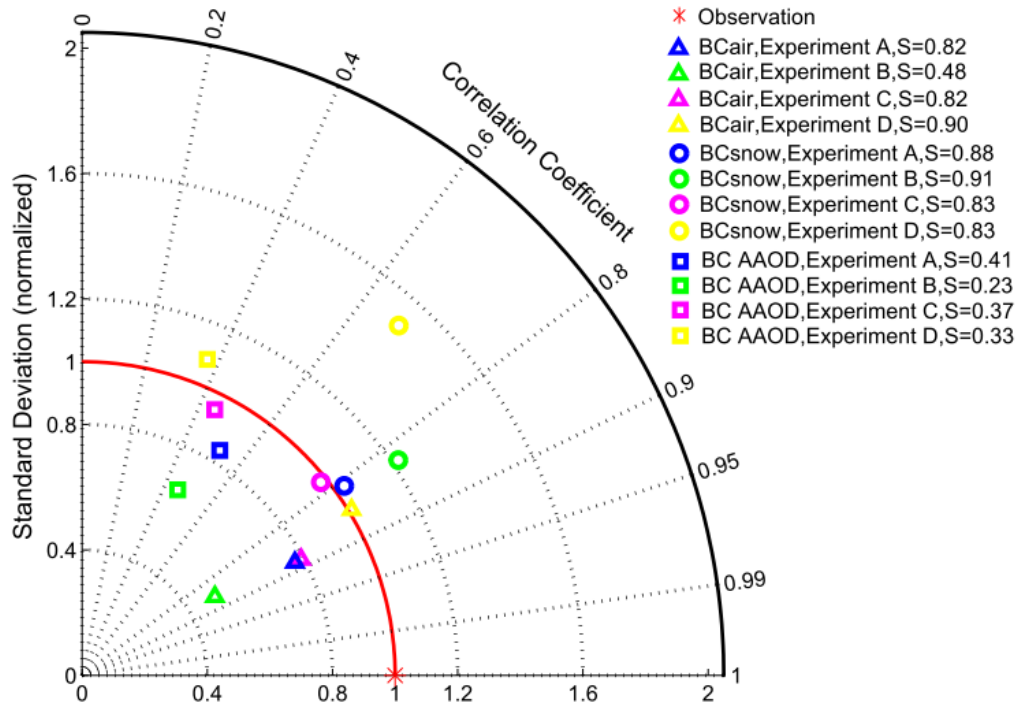


Fig. 10. Taylor diagram of GEOS-Chem simulated versus observed BC concentration in surface air (BC_{air}) and in snow (BC_{snow}), and BC AAOD at sites over the Tibetan Plateau (see Tables 1, 2 and 3 and Fig. 1). Red asterisk is the observation. Triangles, circles and squares, respectively, indicate modeled BC_{air} , BC_{snow} , and BC AAOD from Experiments A (blue), B (green), C (magenta) and D (yellow). See Table 5 and text for more details on the model experiments. Also shown are the Taylor scores (S). Values are for 2006 unless stated otherwise. See text for details.

11

12